Importance of the vegetation-groundwater-stream continuum to understand transformation of biogenic carbon in aquatic systems – A case study based on a pine-maize comparison in a lowland sandy watershed (Landes de Gascogne, SW France)

Loris Deirmendjian, Pierre Anschutz, Christian Morel, Alain Mollier, Laurent Augusto, Denis Loustau, Luiz Carlos Cotovicz, Damien Buquet, Katixa Lajaunie, Gwénaëlle Chaillou, et al.

Importance of the vegetation-groundwater-stream continuum to understand transformation of biogenic carbon in aquatic systems – a case study based on a pine-maize comparison in a lowland sandy watershed (Landes de Gascogne, SW France)

Loris Deirmendjian[1, *], Pierre Anschutz[1], Christian Morel[2], Alain Mollier[2], Laurent Augusto[2], Denis Loustau[2], Luiz Carlos Cotovicz Jr.[1,3], Damien Buquet[1], Katixa Lajaunie[1, 4], Gwenaëlle Chaillou[5], Baptiste Voltz[1, 6], Céline Charbonnier[1], Dominique Poirier[1], and Gwenaël Abril[1, 3, 7]

[1]Laboratoire Environnements et Paléoenvironnements Océaniques et Continentaux (EPOC), CNRS, Université de Bordeaux, Allée Geoffroy Saint-Hilaire, 33615 Pessac Cedex France.

[2] UMR 1391 ISPA, INRA, Bordeaux Sciences Agro, Villenave d'Ornon, 33883 France.

[3]Programma de pos-graduação em Geoquímica, Universidade Federal Fluminense, Outeiro São João Batista s/n, 24020015, Niterói, RJ, Brazil.

[4]Aix Marseille Université, CNRS/INSU, Université de Toulon, IRD, Mediterranean Institute of Oceanography (MIO) UM 110.

[5]Département Biologie, Chimie, Géographie, Université du Québec à Rimouski, Québec, Canada

[6]Univ. Lille, CNRS, Univ. Littoral Côte d'Opale, UMR 8187, LOG, Laboratoire d'Océanologie et de Géosciences, F 62 930, Wimereux, France.

[7]Biologie des Organismes et Ecosystèmes Aquatiques (BOREA), Muséum National d'Histoire Naturelle, CNRS, IRD, UPMC, UCBN, UAG. 61 rue Buffon, 75231, Paris cedex 05, France.

* Now at Chemical Oceanography Unit, University of Liège, Liège, Belgium.

Correspondence to Loris Deirmendjian (Loris.deirmendjian@uliege.be)

Abstract

During land-aquatic transfer, carbon (C) and inorganic nutrients (IN) are transformed in soils, groundwater, and at the groundwater-surface water interface as well as in stream channels and stream sediments. However, processes and factors controlling these transfers and transformations are not well constrained, particularly with respect to land use effect. We compared C and IN concentrations in shallow groundwater and first-order streams of a sandy lowland catchment dominated by two types of land use: pine forest and maize cropland. Contrary to forest groundwater, crop groundwater exhibited oxic

conditions all-year round as a result of higher evapotranspiration and better lateral drainage that decreased the water table below the organic-rich soil horizon, prevented the leaching of soil-generated dissolved organic carbon (DOC) in groundwater, and thus limited consumption of dissolved oxygen (O_2). In crop groundwater, oxic conditions inhibited denitrification and methanogenesis resulting in high nitrate (NO_3^-; on average 1,140 ± 485 µmol L^{-1}) and low methane (CH_4; 40 ± 25 nmol L^{-1}) concentrations. Conversely, anoxic conditions in forest groundwater led to lower NO_3^- (25 ± 40 µmol L-1) and higher CH_4 (1,770 ± 1,830 nmol L^{-1}) concentrations. The partial pressure of carbon dioxide (pCO_2; 30,650 ± 11,590 ppmv) in crop groundwater was significantly lower than in forest groundwater (50,630 ± 26,070 ppmv), and was apparently caused by the deeper water table delaying downward diffusion of soil CO_2 to the water table. In contrast, pCO_2 was not significantly different in crop (4,480 ± 2,680 ppmv) and forest (4,900 ± 4,500 ppmv) streams, suggesting faster degassing in forest streams resulting from greater water turbulence. Although NO_3^-concentrations indicated that denitrification occurred in riparian-forest groundwater, crop streams nevertheless exhibited important signs of spring and summer eutrophication such as the development of macrophytes. Stream eutrophication favored development of anaerobic conditions in crop stream sediments, as evidenced by increased ammonia (NH_4^+) and CH_4 in stream waters and concomitant decreased in NO_3^- concentrations as a result of sediment denitrification. In crop streams, dredging and erosion of streambed sediments during winter sustained high concentration of particulate organic C, NH_4^+ and CH_4. In forest streams, dissolved iron (Fe^{2+}), NH_4^+ and CH_4 were negatively correlated with O_2 reflecting the gradual oxygenation of stream water and associated oxidations of Fe^{2+}, NH_4^+ and CH_4. The results overall showed that forest groundwater behaved as source of CO_2 and CH_4 to streams, the intensity depending on the hydrological connectivity among soils, groundwater, and streams. CH_4 production was prevented in cropland in soils and groundwater, however crop groundwater acted as a source of CO_2 to streams (but less so than forest groundwater). Conversely, in streams, pCO_2 was not significantly affected by land use while CH_4 production was enhanced by cropland. At the catchment scale, this study found substantial biogeochemical heterogeneity in C and IN concentrations between forest and crop waters, demonstrating the importance of including the full vegetation-groundwater-stream continuum when

estimating land-water fluxes of C (and nitrogen) and attempting to understand their spatial and temporal dynamics.

Keywords: carbon dioxide, methane, groundwater, stream, land use, pine, maize

1. Introduction

Despite their small surface area worldwide (Downing et al., 2012), inland waters have been recognized as key component of the global carbon (C) cycle, constituting a preferential pathway of dissolved and particulate C transport from terrestrial ecosystems to the coastal ocean (Cole et al., 2007; Meybeck, 1982; Ludwig et al., 1996b, 1996a; Meybeck, 1987). Inland waters act as significant sources of carbon dioxide (CO_2) and methane (CH_4) to the atmosphere because inland waters are generally supersaturated by CO_2 and CH_4 compared to the overlying atmosphere (Abril et al., 2014; Bastviken et al., 2011; Borges et al., 2015; Lauerwald et al., 2015; Raymond et al., 2013; Stanley et al., 2016).

Inland waters and specifically small streams are tightly connected to their catchment characteristics such as hydrology and land use, as they receive large inputs of C from land (mainly from soils and groundwater), which in turn control the stream biogeochemical processes and the water composition (Aitkenhead et al., 1999; Deirmendjian and Abril, 2018; Hotchkiss et al., 2015; Johnson et al., 2006; Jones and Mulholland, 1998; McClain et al., 2003; Polsenaere and Abril, 2012; Bodmer et al., 2016; Findlay et al., 2001; Lehrter, 2006). Groundwater discharge has been recognized as an important source of CO_2 in riverine systems, especially in small streams and headwaters (Deirmendjian and Abril, 2018; Hotchkiss et al., 2015; Johnson et al., 2008; Kokic et al., 2015; Marx et al., 2017; Raymond et al., 2013; Wallin et al., 2013). On the contrary to riverine CO_2, riverine CH_4 is likely to originate from wetlands that generally combine a strong hydrological connectivity with riverine waters and a high productivity (Abril et al., 2014; Abril and Borges, 2018). Although some studies found low CH_4 concentrations in the groundwater of Belgium (up to 1.1 µmol L^{-1}; Borges et al., 2018; Jurado et al., 2017), other studies found high CH_4

concentrations in the groundwater of Great Britain (up to 295 µmol L^{-1}; Bell et al., 2017) and in the Appalachian basin of the USA (up to 2,8000 µmol L^{-1}; Molofsky et al., 2016). Actually, soil moisture, which controls oxic/anoxic conditions in soil, is the main determinant of terrestrial CO_2 or CH_4 production in soil. As a consequence,CH_4 emissions from soils are high under strictly anaerobic conditions in waterlogged soils whereas CO_2 emissions from soils are high under aerobic conditions in drier soils (Christensen et al., 2003; Moore and Knowles, 1989). Croplands affect water mass balance at the plot scale, especially through irrigation and extraction of groundwater, which results in declining water table in many regions worldwide (Foley et al., 2005; Gleick, 2003; Jackson et al., 2001; Postel, 1999; Rosegrant et al., 2002). Investigating spatial dynamics of CO_2 and CH_4 in groundwater in relation with land use is critical better understanding processes governing their terrestrial production and leaching to groundwater.

Croplands cover about 40% of the terrestrial ice-free surface and are often associated with degradation of both ground and surface water quality (Asner et al., 2004; Clague et al., 2015; Foley et al., 2005; Hiscock et al., 1991; Ramankutty and Foley, 1999). Intensive agriculture led to an increase of nitrate (NO_3^-) entering ground and surface water environments that has fueled aquatic primary production in surface waters and led to low CO_2 and high CH_4 concentrations, the latter being related to enhanced organic matter delivery in sediments (Borges et al., 2018; Carpenter et al., 1998; Clague et al., 2015; Crawford et al., 2016; Jordan and Weller, 1996; Smith, 2003; Zhou et al., 2017). Additionally, aquatic primary production in crop streams is enhanced as a result of low light limitation (clearing of riparian vegetation), and the excessive transport of sediment-bound organic matter and nutrients to surface waters (Bernot et al., 2010; Lamba et al., 2015; Ramos et al., 2015; Young and Huryn, 1999). Soil erosion rates in agricultural landscapes are one to two times larger than those in areas with native vegetation (Montgomery, 2007; Quinton et al., 2010). Indeed, riparian forest is usually considered stream buffer zones that attenuate stream bank erosion and NO_3^- inputs from croplands (Balestrini et al., 2016; Cey et al., 1999; Christensen et al., 2013; Stott, 2005; Wynn and Mostaghimi, 2006). Denitrification represents a permanent removal pathway that limits the extent and impact of NO_3^- contamination by transforming NO_3^-

106 to inert dinitrogen (N_2). However, incomplete denitrification can produced nitrous oxide (N_2O), a major
107 anthropogenic ozone-depleting substance (Ravishankara et al., 2009). On the contrary to croplands, forests
108 are known to export fewer nutrients by limiting runoff and leakage of nutrients (Canton et al., 2012;
109 Onderka et al., 2010).

110 Land use effects on both water composition and biogeochemical processes have been studied in streams
111 and groundwater (Barnes and Raymond, 2010, 2009; Bernot et al., 2010; Bodmer et al., 2016; Jeong,
112 2001; Lehrter, 2006; Masese et al., 2017; Raymond and Cole, 2003; Rodrigues et al., 2018; Salvia-
113 Castellví et al., 2005; Vidon et al., 2008; Wilson and Xenopoulos, 2009; Young and Huryn, 1999; Zhang
114 et al., 2018), but land use studies with simultaneous groundwater and stream sampling are more scarce
115 (Bass et al., 2014; Borges et al., 2018; Hu et al., 2016). The objective of this study was to understand how
116 two contrasting types of land use (pine forest and maize cropland) affected C and inorganic nutrient (IN)
117 concentrations in shallow groundwater and in first-order streams of a sandy lowland catchment. We
118 hypothesized that the biogeochemical variability between crop groundwater and forest groundwater was
119 due to agricultural practices that affect N inputs (fertilizer) and water mass balance (irrigation and
120 drainage). We hypothesized that the biogeochemical variability between crop and forest streams originate
121 from differential lateral export of C and IN from two distinct sources (i.e., crop groundwater and forest
122 groundwater) because of a strong hydrological connection between groundwater and streams in the
123 studied catchment.

124

125 **2. Materials and Methods**

126 **2.1. Study site**

127 The Leyre catchment (2,100 km²) is located in the southwestern part of France. This is a flat coastal plain
128 with a mean slope lower than 0.125% and a mean altitude lower than 50 m (Jolivet et al., 2007). The
129 lithology is relatively homogeneous and composed of sandy permeable surface layers dating from the

130 Plio-Quaternary period (Legigan, 1979; Bertran et al., 2009, 2011). The soils are podzols characterized by
131 a low pH (≈4), low nutrient availability, low cationic exchange capacity, and high organic C content that
132 can reach 50 g per kg of soil (Augusto et al., 2010; Lundström et al., 2000). In Leyre sandy podzols, the
133 low clay and silt content causes a low soil water retention (Augusto et al., 2010).

134 The study area was a vast wetland until the 19th century, when a wide forest of maritime pine was sown
135 following a landscape drainage campaign resulting from an imperial decree of Napoleon III in 1857
136 (Jolivet et al., 2007). Currently, the catchment is mainly occupied by C_3 pine forest (approximately 85%),
137 with a modest proportion of C_4 maize cropland (approximately 15%) (Fig. 1; Jolivet et al., 2007).
138 Following catastrophic forest wildfires, the maize croplands were installed during the second half of the
139 20th century. Consequently, their spatial distribution was not based on soil properties, as confirmed by the
140 similar mean values of soil texture in local croplands and forests (Augusto et al., 2010; Jolivet et al.,
141 2003). During the maize cropping season (usually May to November), farmers irrigate the plots by
142 pumping shallow groundwater (~1-5 m deep) almost daily to maintain adequate soil moisture status,
143 whereas maritime pine stands are never irrigated (Govind et al., 2012). As N is not limiting for tree growth
144 in our study region (Trichet et al., 2009), forests are never fertilized with N. Conversely, croplands
145 generally receive two N fertilizer applications annually, a first at the beginning of May (30–50 kg N ha^{-1}),
146 and second at the beginning of June with 200–250 kg N ha^{-1} (Canton et al., 2012; Jambert et al., 1997;
147 Ulrich et al., 2002). Additionally, in order to maintain soil pH in the 5.5–6.0 range, local maize croplands
148 are limed with crushed limestone ($CaCO_3$) containing a small portion of dolomite ($CaMg(CO_3)_2$) (10 t ha^{-1}
149 right after forest conversion and then 0.5 t ha^{-1} an^{-1}; Jolivet et al., 2003).

150 The climate is oceanic with a mean annual air temperature of 13°C and a mean annual precipitation of 930
151 mm (Moreaux et al., 2011). Owing to the low slope, the low soil water retention and the high permeability
152 of the soil (i.e., hydraulic conductivity is approximately 40 cm h^{-1}, Corbier et al., 2010), the percolation of
153 rain water is fast (55 cm h^{-1} on average, Vernier and Castro, 2010). Consequently, surface runoff does not
154 occur as the excess of rainfall percolates into the soil and recharges the shallow groundwater, causing the

155 water table to rise. The sandy permeable surface layers contain a free and continuous water table that is
156 strongly interconnected with the superficial river network. This is facilitated by a dense network of
157 drainage ditches, initiated in the 19th century and currently maintained by forest managers in order to
158 enhance tree regeneration and growth (Thivolle-Cazat and Najar, 2001). During the sampling period,
159 channels of some crop streams were dredged before they began to flow again. This was done to optimize
160 local cropland drainage and to feed croplands with IN and organic residuals found in the stream
161 sediments. To increase soil permeability and to optimize lateral drainage in local maize croplands, farmers
162 practice subsoiling and agricultural ditches are generally deeper (2.0–2.5m) than forest ditches (1.0m).

163

164 **2.2. Sampling strategy**

165 We defined order 0 as groundwater and order 1 as streams and ditches either having no tributaries or being
166 seasonally dry (from June to December during our sampling period). We selected 17 sampling stations (5
167 shallow groundwater and 12 first-order streams) within the Leyre catchment (Tab. 1; Fig. 1). The
168 groundwater sampling stations were located in maize cropland (n=2), pine forest (n=2; one is the Bilos
169 station (FR-Bil) of the ICOS Research infrastructure) and in a riparian forest adjacent to a maize cropland
170 (n=1; Tab. 1; Fig. 1). The stream sampling stations were chosen based on the different proportions of
171 croplands in their respective catchments (Tab. 1; Fig. 1).

172 Groundwater was sampled for temperature, electrical conductivity (EC), pH, dissolved oxygen (O_2),
173 methane (CH_4), partial pressure of CO_2 (pCO_2), total alkalinity (TA), dissolved inorganic carbon (DIC),
174 stable isotope composition of the dissolved inorganic carbon (δ^{13}C-DIC), dissolved organic carbon
175 (DOC), ammonia (NH_4^+), nitrate (NO_3^-) and dissolved iron (Fe^{2+}). For groundwater, we took the
176 precaution to renew the water in the piezometers by pumping with a submersible pump before sampling.
177 Groundwater was then sampled once the stabilization (approximately 10 min) of groundwater
178 temperature, pH, EC and O_2 monitored with portable probes was observed. Streams were sampled for the

same parameters, plus total suspended matter (TSM), particulate organic carbon (POC) and the POC content of the TSM (POC%).

2.3. Field measurements and laboratory analyses

Groundwater and streams were sampled at approximately monthly time intervals between Jan. 2014 and Jul. 2015 (Tab. S1). In total, throughout the sampling period, we sampled 55 groundwaters and 137 stream waters.

The pCO_2 in groundwater and streams was measured directly using an equilibrator (Frankignoulle and Borges, 2001; Polsenaere et al., 2013) following the procedure of Deirmendjian and Abril (2018).

We stored the total alkalinity (TA) samples in polypropylene bottles after filtration using a syringe equipped with glass fiber filters (GF/F; 0.7 µm). TA was then analyzed on filtered samples by automated electro-titration on 50 mL samples with 0.1N HCl as the titrant. The equivalence point was determined from pH between 4 and 3 with the Gran method (Gran, 1952). Precision based on replicate analyses was better than ±5 µmol L^{-1}. For samples with a very low pH (<4.5), we bubbled the water with atmospheric air in order to degas the CO_2. Consequently, the initial pH increased above 5, and the TA titration was then performed (Abril et al., 2015).

We calculated DIC from pCO_2, TA, and temperature measurements using the carbonic acid dissociation constants of Millero (1979) and the CO_2 solubility from Weiss (1974), using the CO_2SYS software (Lewis et al., 1998). The δ^{13}C-DIC samples were collected using 120 mL glass serum bottles sealed with a rubber stopper and treated with 0.3 mL of $HgCl_2$ at 20 g L^{-1} to avoid any microbial respiration during storage. Vials were carefully sealed such that no air remained in contact with samples and were stored in the dark to prevent photo-oxidation. The δ^{13}C-DIC measurements were performed with the headspace technique using an isotope ratio mass spectrometer coupled to an elemental analyser (EA-IRMS, Micromass IsoPrime) equipped with a manual gas injection port as described in Gillikin and Bouillon (2007).

203 CH_4 was also measured using a headspace technique in 60 mL glass serum bottles. The headspace was
204 created with 10 mL of N_2 gas. We then injected 0.5 mL of the headspace in a gas chromatograph equipped
205 with a flame ionization detector (GC-FID).

206 DOC samples were obtained after filtration in the field through pre-combusted GF/F (0.7 µm). DOC
207 filtrates were stored in pre-combusted Pyrex vials (25 mL), acidified with 50 µL of 37% HCl to reach pH
208 2, and kept at 4 °C in the laboratory before analysis. The DOC concentrations were measured with a
209 SHIMADZU TOC 500 analyzer (in TOC-IC mode), using a technique based on thermal oxidation after a
210 DIC removal step (Sharp, 1993). The repeatability was better than 0.1 mg L^{-1}.

211 The water for TSM and POC measurements was filtered through pre-weighed and pre-combusted GF/F
212 glass fiber filters (0.7 µm). The filters were dried at 60 °C and stored in the dark, and subsequently, TSM
213 was determined by gravimetry. POC was measured using the same filter. The filters were acidified in
214 crucibles with 2N HCl to remove carbonates and were then dried at 60 °C to remove inorganic carbon and
215 most of the remaining acid and water (Etcheber et al., 2007). POC content was measured by combustion
216 (1500 °C) using a LECO CS 200 analyzer and the CO_2 formed was determined quantitatively by infrared
217 absorption. POC in µmol L^{-1} and POC% were then calculated. The uncertainty was ±0.05% of TSM.

218 For IN determination, water was filtered through a 0.20 µm cellulose acetate syringe membrane.
219 Subsamples for Fe^{2+} were acidified with 37% HCl to prevent precipitation of iron oxide, whereas
220 subsamples for $NH_4^+$and NO_3^- were not acidified but kept frozen until later analyses. Then, NH_4^+, NO_3^-,
221 and Fe^{2+} were analyzed by colorimetry according to standard techniques. NH_4^+ was analyzed following the
222 procedure of Harwood and Kühn (1970). NO_3^- was analyzed by flow injection analysis following the
223 procedure of Anderson (1979). Fe^{2+} was analyzed using the ferrozine method (Stookey, 1970). Precision
224 was ±10% for NH_4^+ and NO_3, and was ±5% for Fe^{2+}.

225 EC, temperature, O_2, and pH were measured using portable probes (WTW®). Before each field trip, the
226 pH probe was calibrated using two NBS buffer solutions (4 and 7), the oxygen polarographic probe was

calibrated to 100% in a humid atmosphere and the conductivity probe was calibrated using a salinity standard.

2.4. Statistical analyses

K-means clustering analysis (MacQueen, 1967) was used to classify waters either as forest-dominated or as cropland-affected (Tab. 1). Indeed, K-means clustering analysis allows partitioning a dataset into k groups (i.e., clusters) pre-specified by the analyst (MacQueen, 1967). Contrary to forest waters at our study site, crop waters exhibit disproportionately higher NO_3^- concentration as a result of N fertilizer use on maize cropland (Canton et al., 2012; De Wit et al., 2005; Jambert et al., 1997, 1994). Consequently, in the K-means clustering analysis we used NO_3^- concentration data as a proxy to establish a statistical distinction between forest and crop waters (Tab. 1). K-means clustering analysis was performed one time with the groundwater dataset (but excluding the riparian groundwater) and a second time with the first-order streams dataset. We excluded data from riparian groundwater because we have considered riparian groundwater as a cluster itself (Tab. 1).

Principal component analysis (PCA) was used to condense multivariate information on correlated biogeochemical parameters to a set of uncorrelated variables called principal components (further referred to as dimensions). PCA was performed one time with a dataset consisting of each measured parameter in groundwater (but excluding the riparian groundwater) and a second time with the corresponding first-order streams dataset. PCA was performed separately for groundwater and streams because particulate parameters were not present in groundwater. If PCA were not performed separately for groundwater and streams, all data from groundwater would have been removed from the analysis (indeed, if one parameter is missing for a given sampling station, the sampling station is entirely deleted from the PCA). In addition, performing the PCA separately for groundwater and streams led to information that was more robust with respect to the biogeochemical variability induced by land use, in either groundwater or streams. However,

to observe whether the two groundwater (crop and forest) and two streams (crop and forest) sources could be distinguished mathematically in one PCA, we performed an additional PCA with data from both groundwater and streams that excluded particulate parameters from the analysis. All concentrations data were log-transformed prior to PCA. The PCAs showed the biogeochemical variability across forest, cropland, and hydrological seasons in either groundwater or first-order streams.

Later, non-parametric bivariate analyses (Mann-Whitney statistical tests) were used to estimate if hydrological seasons or increasing stream order significantly influenced the concentration of a biogeochemical parameter. Linear regressions were performed to model the relationships between two variables by fitting a linear equation to observed data.

K-means clustering analysis (package Stats) and PCA analysis (package FactoMineR for analysis and package factoextra for visualization; Kassambra and Mundt, 2017; Lê et al., 2008) were performed with R software version 3.1.4 (R Core Team, 2018). Mann-Whitney tests and linear regressions were performed with Graph Pad Prism version 7 software.

3. Results

3.1. Hydrology

In previous work based on the same dataset, but excluding cropland sampling stations, we identified two major hydrological seasons (Deirmendjian and Abril, 2018). One defined a high flow period as two relatively short flood events that occurred in Jan. 2014–Mar. 2014 and in Feb. 2015–Mar. 2015, whereas we defined the base flow period as two longer periods of low flow occurring in Apr. 2014–Jan. 2015 and Apr. 2015–Jul. 2015. During high flow, the average and the maximum river flows were 50 $m^3 s^{-1}$ and 119 $m^3 s^{-1}$, respectively. During base flow, the average and the minimum river flow were 10 $m^3 s^{-1}$ and 5 $m^3 s^{-1}$, respectively. The water tables in the forest, riparian forest, and cropland exhibited similar temporal fluctuations but with a different intensity, and the forest had an overall higher water table depth than the

cropland (Fig. 2). The water table in the riparian area exhibited intermediate depth between the forest and cropland sites (Fig. 2). As surface runoff was negligible in the studied sandy and flat catchment, most of the stream water likely originated from groundwater discharge.

To investigate the temporal variability of the studied biogeochemical parameters, we chose to rely on hydrological regimes (high flow and base flow periods) rather than on temperature periods (seasons). At our study site climate was oceanic (by definition very temperate) and the amplitude of the water temperature was not as high as the amplitude of the river flow. As an example, Leyre River (main stem) flow could be up to 119 $m^3 s^{-1}$ and could be down to 5 $m^3 s^{-1}$, whereas the highest water temperature amplitude occurred in forest streams and was 6.4–25.8 °C (Tab. 2). Additionally, most of the lateral export occurred during the short periods of high flow (up to 90% for DOC, Deirmendjian et al., 2018). Thus, characterizing biogeochemical variability and biogeochemical processes in relation with land use during this hydrological period was important. Furthermore, the seasonality induced by water temperature was to a certain extent included in the defined hydrological regimes since the high flow period was associated with lower water temperatures while the base flow period was associated with higher water temperatures (Tabs. 2-4).

3.2. K-means clustering analysis

For both hydrological seasons (i.e., high and base flow), we partitioned each sampling stations (excepting riparian groundwater), into either cropland-affected or forest-dominated waters (Tab. 1). K-means clustering analysis produced satisfactory results. Logically, groundwater located in cropland was classified as crop water whereas groundwater located in forest was classified as forest water (Tab. 1). Stream sampling stations having more than 30% of croplands in their respective catchment were always classified as crop waters (Tab. 1). Stream sampling stations having less than 8% of croplands in their respective catchment were always classified as forest waters excepting two times (Tab. 1). These two stream

sampling stations were located a few kilometers downstream from important maize croplands. Specifically, one station was a ditch strongly vegetated during the base flow period that showed signs of N fertilizer uptake from upstream cropland and, therefore, this ditch was logically classified as a crop station during base flow (Tab. 1). One station was a stream that exhibited a high water flow during the high flow period, which probably increased the upstream cropland influences during this hydrological period and, therefore, this stream was logically classified as a crop station during high flow (Tab. 1).

Excepting one strictly forested headwater, the other sampled streams were not strictly forested or cropped (Tab. 1). Consequently, as explained further, some biogeochemical variability between forest and crop streams was introduced by simple water mixing from two distinct sources: forest groundwater and crop groundwater. We used the term crop stream to indicate a stream classified as a crop-affected one, although such stream was a forest stream affected by cropland rather that a strictly crop stream.

3.3. Land use influence on water composition of shallow groundwater

PCA on the groundwater dataset revealed that groundwater biogeochemical variability was strongly dependent on land use (maize cropland vs. pine forest) and hydrological seasons (base flow vs. high flow) (Figs. 3a, b). The first three PCA dimensions covered 44%, 17.5% and 10.5% of the total variance within the dataset, respectively (Figs. 3a, b).

PCA dimension 1 clearly separated forest groundwater from crop groundwater based on two groups of variables negatively correlated with one another (Fig. 3a). One group of variables was characterized crop groundwater and was composed of EC, NO_3^-, δ^{13}C-DIC, and O_2, whereas the second group of variables was characterized forest groundwater and was composed of DIC, pCO_2, CH_4, Fe^{2+}, and NH_4^+ (Fig. 3a). Indeed, we observed that the yearly average of EC (+270 µS cm^{-1}), NO_3^- (+1,115 µmol L^{-1}), δ^{13}C-DIC (+6.9‰), and O_2 (+200 µmol L^{-1}) were higher in crop groundwater than in forest groundwater and were significantly and positively affected by cropland cover (Tab. 2; Figs. 4b, c, f, j). Conversely, we observed

higher DIC (+1,010 µmol L^{-1}), pCO_2 (+19,985 ppmv), CH_4 (+1,730 µmol L^{-1}), Fe^{2+} (+14.1 µmol L^{-1}), and NH_4^+ (+4.1 µmol L^{-1}) in forest groundwater than in crop groundwater; these were significantly and positively affected by forest cover (Tab. 2; Figs. 4d, e, g, h, k). In riparian groundwater, EC, NO_3^-, δ^{13}C-DIC, O_2, DIC, pCO_2, and CH_4 exhibited intermediate values between the groundwater of forest and crop sites, whereas Fe^{2+} and NH_4^+ were low and close to those found in crop groundwater (Tab. 2; Figs. 4b, c, d, e, f, g, h, j, k).

In crop groundwater, EC, NO_3^-, δ^{13}C-DIC, and O_2 were not significantly affected by hydrological seasons (Figs. 3a, S2c, h, j, k, l). However, δ^{13}C-DIC (+1.1‰), NO_3^- (+120 µmol L^{-1}), and DOC (+130 µmol L^{-1}) were slightly higher (but not significantly) during base flow compared to high flow (Tab. 3; Figs. S2c, h, j, k, l). In forest groundwater, pCO_2, DIC, CH_4, and DOC were significantly affected by hydrological seasons (Tab. 3; Figs. S2g, h, k, l). DOC (+1,490 µmol L^{-1}) was significantly higher during high flow, whereas pCO_2 (+30,980 ppmv), DIC (+1,330 µmol L^{-1}) and CH_4 (+1,780 nmol L^{-1}) were significantly higher during base flow (Tab. 3; Figs. S2 and S4g, h, k, l). In crop and riparian groundwater, we also observed higher pCO_2 and DIC values during base flow, but with lower intensities than in forest groundwater (Tab. 3; Figs. S2h, k).

3.4. Land use influence on water composition of first-order streams

Figures 3c-d present PCA based on first-order streams data set. The first three PCA dimensions covered 28.6%, 18.5% and 13.8% of the total variance within the dataset, respectively (Figs. 3c, d).

Interestingly, the PCA based on the first-order streams dataset did not clearly separate crop streams from forest streams as it did for groundwater dataset (Figs. 3a-d). This implied lower spatial variability in streams in relation to land use in than in groundwater (Tabs. 2-4; Fig. 4). Nevertheless, a land use gradient was observed on PCA dimension 2 (Figs. 3c, d). PCA dimension 2 was best defined by a group of variables composed of EC, CH_4, NO_3^-, NH_4^+, DOC, TSM, and POC, which collectively characterized crop

347 streams (Figs. 3c, d). On a yearly average basis, significantly higher EC (+105 µS cm^{-1}), CH_4 (+220 µmol
348 L^{-1}), NO_3^- (+265 µmol L^{-1}), NH_4^+ (+4.3 µmol L^{-1}), DOC (+135 µmol L^{-1}), TSM (+3.3 mg L^{-1}), and POC
349 (+70 µmol L^{-1}) were observed in crop streams compared to forest streams (Tab. 2; Figs. 4b, c, d, g, l, m,
350 o). High CH_4, NH_4^+, and DOC concentrations were characteristics of forest groundwater, but in streams,
351 these parameters were characteristic of crop streams (Figs. 3a-d). In addition, pCO_2, DIC, δ^{13}C-DIC and
352 O_2 were not able to separate crop streams from forest streams as they did for groundwaters (Figs. 3a-d).
353 On a yearly average basis, no significant differences were observed between crop and forest streams for
354 these four parameters (Figs. 3f, h, j, k).

355 The relatively low temporal variability between high and base flow periods observed in both crop and
356 forest streams for the studied parameters did not allow the PCA based on stream data set to clearly
357 separate base flow samples from high flow samples (Tab. 4; Figs. 3c-d, S3, S4). Nevertheless, in crop
358 streams, pH (+0.2) and δ^{13}C-DIC (+3.8‰) were significantly higher during base flow while pCO_2 (-1,160
359 ppmv), NO_3^- (-130 µmol L^{-1}) and DOC (-230 µmol L^{-1}) were significantly lower during the same period
360 (Tab. 4; Figs. S3a, j, c, h, l, m, o). In streams, TSM and POC were significantly higher during high flow
361 but with a higher intensity in crop streams than in forest streams (Tab. 4; Fig. S3m, o). Interestingly, in
362 both forest and crop streams, POC% was not significantly affected by hydrological regime (Tab. 4; Fig.
363 S3n).

364

365 **3.5. Upstream-downstream distribution of biogeochemical parameters**

366 To explore the influence of land use on water composition at the groundwater-stream continuum, we
367 observed the upstream-downstream (groundwater-stream) distribution of biogeochemical parameters
368 along forest and crop continuums (Tab. 2; Fig. 4). Along both types of continuum, some parameters (i.e.,
369 pCO_2, TA, DIC, δ^{13}C-DIC, pH, O_2) exhibited the same upstream-downstream distribution, whereas other

parameters (i.e., EC, NO_3^-, NH_4^+, Fe^{2+}, CH_4, DOC) exhibited a different upstream-downstream distribution (Tab. 2; Fig. 4).

In crop and forest continuums, we observed strong spatial patterns for pCO_2, TA, DIC, δ^{13}C-DIC, and pH: pCO_2 and DIC decreased while TA remained more or less constant, and δ^{13}C-DIC and pH increased (Tab. 2; Figs. 4a, h, i, j, k). However, a larger decrease in pCO_2 levels in the forest continuum suggested a more intense degassing in forest streams (Tab. 2; Fig. 4h). We also observed an increase in O_2 in both types of continuum, which could result from stream ventilation, although with a higher intensity in forest continuum (Tab. 2; Figs. 4f, h).

EC decreased downstream in the crop continuum, but did not in the forest continuum where EC remained very stable and much lower than in the crop continuum (Tab. 2; Fig. 4b). NO_3^- decreased downstream between groundwater and streams in croplands, and in contrast, in forests NO_3^- increased downstream between groundwaters and streams (Tab. 2; Fig. 4c). NH_4^+, Fe^{2+}, and CH_4 decreased in the forest continuum but they increased in the crop continuum (Tab. 2; Figs. 4d, e, g). DOC significantly decreased in the forest continuum but remained stable in the crop continuum (Tab. 2; Fig. 4l). TSM and POC were significantly higher in crop relative to forest streams; however, similarly high POC% (28%) was observed in both types of streams (Tab. 2; Fig. 4m, n, o).

3.6. Biogeochemistry dynamics in the groundwater-stream continuum

PCA with groundwater and streams datasets indicated mathematically that streams were fed with two distinct sources: forest groundwater mostly characterized by high pCO_2, DIC, and CH_4 concentrations and crop groundwater mostly characterized by high NO_3^- concentrations (Figs. 5). Forest and crop streams were characterized by higher O_2, δ^{13}C-DIC and pH values than in groundwater (Figs. 5). In this PCA, the distinction between forest and crop streams was primarily a function of NO_3^-, crop streams points were moved upward along dimension 2 (Figs. 5). Throughout the sampling period, we observed a negative

linear relationship (R^2=0.6, p<0.001, n=192) between CO_2 and O_2 for all sampled groundwater and streams (Fig. 6a). On the one side, stream samples were mostly characterized by high O_2 (mean was 290 µmol L^{-1}) and low CO_2 (mean was 4,480 ppmv), excepting some forest streams during summer that were characterized by low O_2 (down to 110 µmol L^{-1}) and high CO_2 (up to 27,200 ppmv) (Tab. 2; Figs. 6a, S4f, h). On the other side, anoxic conditions associated with high CO_2 (mean was 50,630 ppmv) were characteristic of forest groundwater, whereas crop groundwater exhibited O_2 (mean was 220 µmol L^{-1}) and CO_2 (mean was 30,650 ppmv) intermediate between streams and forest groundwater (Tab. 2; Fig. 6a). In forest groundwater, DOC was negatively and linearly correlated with CO_2 (R^2=0.4, p <0.001, n=22) suggesting that part of groundwater CO_2 came from degradation of groundwater DOC (Fig. 6b). A comparison of CO_2 and CH_4 for all sampled groundwaters and streams showed that a large portion of the CO_2 and CH_4 in forest streams could come from forest groundwater discharge (Tab. 2; Fig. 6e). In crop streams, CH_4, NH_4^+, and Fe^{2+} could not originate from crop groundwater discharge since they had much lower CH_4, NH_4^+, and Fe^{2+} concentrations than crop streams (Tab. 2; Fig. 6e, 7e, 7f). We observed a positive linear relationship between CH_4 and NH_4^+ (R^2=0.4, p<0.001, n=53) in crop streams, demonstrating that these two compounds may come from the same source (Fig. 7d). Conversely, a comparison of O_2 and NH_4^+ or Fe^{2+} in forest streams indicated that NH_4^+ and Fe^{2+} were mostly discharged through forest groundwater (Fig. 7e, f). In forest streams, the negative linear relationship between O_2 and NH_4^+ (R^2=0.1, p-value<0.05, n=70), Fe^{2+} (R^2=0.5, p-value<0.001, n=77), or CH_4 (R^2=0.1, p-value<0.001, n=77) suggested oxidation of these reduced compounds in the stream water column (Fig. 7e, f). We observed a gradient of NO_3^- concentration, from high values to low values, between crop groundwater (mean was 1,140 µmol L^{-1}), to riparian groundwater and crop streams (310 and 340 µmol L^{-1}, respectively), to forest streams (75 µmol L^{-1}) and to forest groundwater (25 µmol L^{-1}) (Tab. 2; Fig. 7a, b, c). In crop streams, a large share of riverine NO_3^- could be discharged through crop groundwater. Conversely, NO_3^- concentration in forest streams could not be explained by NO_3^- concentration in forest groundwater (Tab. 2; Fig. 7a, b, c, d). In crop groundwater, high NO_3^- concentrations were associated with

low CH_4 concentrations. In crop streams, high NO_3^- concentrations could be related to high CH_4 concentrations (Fig. 7c).

4. Discussion

4.1. Water table depth in relation to land use

At the studied catchment scale, lithology, topography, soils, and precipitation are more or less uniform (Augusto et al., 2010; Jolivet et al., 2003). At the plot scale, spatial variability of water table depth in relation to land use was thus necessarily dependent on how water outputs (drainage, evapotranspiration or groundwater storage) of the water mass balance were human-affected (Govind et al., 2012; Stella et al., 2009). Local forests are never irrigated, conversely, irrigation with extraction of groundwater (that decreases groundwater storage) in local croplands could strongly bias the water mass balance at the plot scale since about half of the water diverted for irrigation is rapidly consumed through evapotranspiration (e.g., Jackson et al; 2001). Additionally, evapotranspiration in maize croplands is typically higher than in forests owing to the larger stomatal conductance that makes the exchange of C and water between the biosphere and the atmosphere much easier (Govind et al., 2012; Stella et al., 2009). Other studies have shown that the combination of subsoiling practices (increasing soil permeability) with deep agricultural ditches in croplands also affected water mass balance at the plot scale by enhancing lateral drainage of groundwater (Evans et al., 1996; Robinson et al., 1985). From an 8 year survey of local cropland, Juste et al (1982) showed that lateral drainage strongly affected the water mass balance at the plot scale as it represented an annual mean of 637 mm (70% of the amount of precipitation), whereas precipitation was estimated at 922 mm. At the forest plot scale, lateral drainage represented an annual mean of 182 mm (20% of the amount of precipitation), whereas precipitation was estimated at 895mm (Deirmendjian et al, 2018). At the study site, deeper water table in croplands was thus a consequence of a higher evapotranspiration and more lateral drainage than in forest. As explained further, water table depth is an

443 important determinant for understanding the biogeochemical variability in groundwater in relation to land
444 use.

445

446 **4.2. Dynamic of O_2, DOC, DIC and δ^{13}C-DIC in groundwater: a combination of hydrological,**
447 **physical and metabolic processes**

448 In other aquifer systems worldwide, several studies have observed a significant positive correlation
449 between groundwater O_2 concentration and depth to water (Datry et al., 2004; Foulquier et al., 2010;
450 Goldscheider et al., 2006; McMahon and Chapelle, 2008; Pabich et al., 2001). Where the water table is
451 close to the soil surface, groundwater O_2 consumption is likely rapid because of incomplete degradation of
452 soil-generated labile DOC in the unsaturated zone. On the contrary, where the water table is far from the
453 soil surface, strong oxygen depletion in the vicinity of the water table does not occur since the higher
454 residence time of infiltrating water results in almost complete degradation of soil-generated DOC in the
455 unsaturated zone (Malard and Hervant, 1999; Starr and Gillham, 1993). A regional study in forest soils of
456 Switzerland (Hagerdon et al., 2000) and a study compiling a global database of soil carbon (Camino-
457 Serrano et al., 2014) both found that soil-generated DOC was preferentially mobilized under reducing
458 conditions in soils because of dissolution of Fe oxides. Deeper water tables in croplands do not reach
459 topsoil that exhibits high labile organic C content. Thus, reducing conditions in topsoil and the leaching of
460 soil-generated DOC are prevented as is the consumption of the groundwater O_2 stock, as occurs in forests
461 during high flow stages (Tab. 3; Fig. S2l; Deirmendjian et al. 2018). Therefore, groundwater pCO_2 was
462 higher in the forest during high flow than it was in cropland and riparian sites (Tab.3; Figs. 4h, S2l, h).
463 This also explains the negative correlation between DOC and CO_2 observed only in forest groundwater
464 (Fig. 6b). During base flow, we observed a clear land use spatial pattern among cropland, riparian forest,
465 and forest sites (Tab. 3; Fig. S2h). We hypothesize that this difference was a consequence of a less intense
466 soil respiration in croplands during summer. From simultaneous eddy covariance measurements over pine
467 forests and maize croplands of the study area, Stella et al (2009) confirmed that ecosystem respiration was

lower in croplands than in forests over the whole year. However, Stella et al (2009) also showed that ecosystem respiration was larger during the growing season of the maize, because of increased of soil respiration in response to the higher soil water content caused by irrigation. In forest sites, groundwater pCO_2 increases during the summer because soil CO_2 diffuses downward and then is dissolved into the water table (Deirmendjian et al., 2018; Tsypin and Macpherson, 2012). A deeper water table in cropland suggests a less efficient CO_2 transfer from soil air to water table. Higher soil moisture in croplands due to irrigation probably delays soil CO_2 diffusion to groundwater.

The δ^{13}C-DIC signature of forest groundwater was typical of a signature that originated from respiration of soil organic matter derived from C_3 plants (O'Leary, 1988; Vogel et al., 1993). The studied forest soils have no natural carbonate minerals (Augusto et al., 2010) and DIC originating from silicate weathering has the same isotopic signature as DIC originating from soil respiration (Das et al., 2005; Polsenaere and Abril, 2012; Wachniew, 2006). Crop groundwater had a heavier δ^{13}C-DIC signature than forest groundwater and this discrepancy resulted from distinct processes. Liming in cropland brings artificial carbonates into crop soil and DIC originating from carbonate weathering produced DIC with a δ^{13}C value of approximately half of that of soil CO_2 as carbonate rocks have a δ^{13}C of approximately 0 ‰, making δ^{13}C-DIC less negative (Clark and Fritz, 1997; Salomons and Mook, 1986). Irrigation with extraction of groundwater could also increase the δ^{13}C-DIC signature by enhancing the degassing rate of $^{12}CO_2$ relative to $^{13}CO_2$ (Deirmendjian and Abril, 2018; Polsenaere and Abril, 2012). Changes in the δ^{13}C-DIC signature could also originate from respiration of soil organic matter derived from maize, a C_4 plant with a heavier δ^{13}C signature than C_3 forest plants (O'Leary, 1988; Vogel et al., 1993), as observed in the study region (Quénéa et al., 2006). Indeed, after three decades of cultivation, the remaining carbon from the forest pool was mostly recalcitrant and its degradation probably did not affect the δ^{13}C-DIC pool (Jolivet et al., 1997).

4.3. Dynamics of IN and CH_4 in groundwater: the influence of groundwater O_2

Subsurface and groundwater redox zonation is driven by the spatial and temporal distribution of O_2 that serves as the primary terminal electron acceptor during the degradation of organic C. In crop groundwater, high O_2 concentrations inhibited methanogenesis, as this process is strictly anaerobic and thus resulted in very low CH_4 concentrations (Tab. 2; Figs. 4f, g; Borges et al., 2018; Ciais et al., 2010; Jurado et al., 2017; Klüber and Conrad, 1998). Conversely, forest and riparian groundwater exhibited anoxic conditions that allowed methanogenesis to occur and created higher CH_4 concentration in forest sites compared to cropland sites (Tab. 2; Figs. 4f, g). High water table stages in forested areas cause anoxia in soils, forcing plants and microorganisms to switch to anaerobic metabolism (Naumburg et al., 2005; Bakker et al., 2006, 2009). Thus, in riparian and forest areas, we expected a positive relationship between water table and groundwater CH_4 but, to the contrary, we observed a negative relationship between these two parameters ($R^2 = 0.25$, $p<0.05$; data not shown). This implies that methanogenesis primarily occurs in deeper layers of forest soils, especially in summer. Fe^{2+} and NH_4^+ accumulates in forest groundwater because anoxic conditions inhibit nitrification and iron oxidation (Tab. 2; Figs. 4d, e; Jambert et al., 1994; Widdel et al., 1993).

In groundwater, anoxic conditions enable heterotrophic denitrification, whereas an O_2 threshold of 30–60 µmol L^{-1} completely inhibits heterotrophic denitrification (Balestrini et al., 2016; Cey et al., 1999; Christensen et al., 2013; Jambert et al., 1994; Kolbjørn Jensen et al., 2017; Korom, 1992). In strictly forest sites, denitrification in groundwater is usually limited by the scarcity of NO_3^-, whereas in strictly crop sites denitrification is often limited by organic C availability (Tab. 2; Jambert et al., 1994; Starr and Gillham, 1993). Thus, N fertilizer application associated with different groundwater denitrification rates in the different plots creates the observed spatial pattern of groundwater NO_3^- concentration in crop, riparian and forest sites (Tab. 2; Fig. 4c). In local maize croplands, Jambert et al (1997) found that 13% of the N fertilizers inputs were converted to N_2 gas, demonstrating that denitrification could occur in these oxic crop soils and groundwater. Although oxic conditions are not favorable for groundwater denitrification, some studies in agricultural catchments do describe this process at relatively high O_2 (150 µmol L^{-1})

levels (McAleer et al., 2017; Otero et al., 2009). In crop soils, Rubol et al. (2016) investigated the spatio-temporal dynamics in oxidative microbial activity and the development of anoxic micro zones (i.e., anoxic hot-spots) at the microscopic level (μm to cm). They found that labile C addition resulted in maximum rates of local metabolic activity within a few minutes and led to the subsequent formation of anoxic hotspots and thus, both oxic and anoxic conditions coexisted closely within a small volume of crop soils. Consequently, denitrification probably occurs in anoxic microsites in waterlogged soil during irrigation as higher soil moisture results in lower soil oxygen concentration, lower redox potential and higher leaching of soil DOC (Hagedorn et al., 2000; Jambert et al., 1997; Rubol et al., 2012; Silver et al., 1999).

N fertilizer load in local croplands is 25 g N m^{-2} yr^{-1} (Jambert et al., 1997), whereas export (using drainage of 637 mm yr^{-1} and the average NO_3^- concentration in crop groundwater) of NO_3^- through crop groundwater was estimated at 10 g N m^{-2} yr^{-1} (40% of the annual N fertilizer load), and export (using same drainage and the average NO_3^- concentration in riparian groundwater) of NO_3^- through riparian groundwater was estimated at 2.8 g N m^{-2} yr^{-1} (8% of the annual N fertilizer load). This shows the importance of riparian groundwater to attenuate N inputs from adjacent croplands to streams, otherwise a large portion of the annual N fertilizer load would have been leached into adjacent streams rather than being denitrified or used by plants. In riparian groundwater adjacent to a farm in the New York state (USA), Anderson et al. (2014) found that total groundwater denitrification was equivalent to 32% of manure N spread on the adjacent upland field. (Mekala et al., 2017) simulated the transport and dynamics of N in an agricultural soil under flooded conditions and concluded that relatively shallow aquifers with sandy soil are vulnerable to NO_3^- contamination at around 10 days if continuous irrigation is practiced. They also stated that NO_3^- had higher leaching potential than NH_4^+ or DOC. At our study site, irrigation and associated desorption of DOC and NO_3^- could explain their slight increase in crop groundwater during base flow (Tab. 3, Figs. 1, S2c). In a storm infiltration basin in Florida (USA), O'Reilly et al. (2012) found that concomitant peaks in groundwater O_2 and NO_3^-concentrations after storm rainfall were a consequence of organic N leaching, indicating that there were short periods of ammonification and

nitrification. In crop groundwater of Wallonia (Belgium), when groundwater O_2 levels are higher than 125 µmol L^{-1} (as at the study site), nitrification rather than denitrification promotes the accumulation of N_2O in groundwater (Jurado et al., 2017).

4.4. Stream biogeochemical functioning: mostly a function of groundwater composition

NO_3^- inputs to streams cause stream eutrophication (Carpenter et al., 1998; Jordan and Weller, 1996; Smith, 2003; Zhou et al., 2017). This is consistent with our field observations where we observed that crop streams were highly vegetated with macrophytes during base flow stages. Compared to high flow conditions, crop stream eutrophication was accompanied by higher pH and δ^{13}C-DIC, and lower pCO_2caused by preferential $^{12}CO_2$ uptake during the macrophyte plant photosynthesis (Tab. 4; Figs. S3a, h, j; De Carvalho et al., 2009; Raven et al., 2002). The development of macrophytes in crop streams modifies flow and can cause a significant drop in water velocity, which in turn, gives rise to extensive deposition and retention of sediment beneath the macrophytes (Cotton et al., 2006; Sand-Jensen and Pedersen, 1999). This leads to seasonal accumulation of organic matter, a predominance of anoxic conditions in stream sediments, and thus the occurrence of methanogenesis as evidenced by peaks in dissolved CH_4 during base flow (Tab. 4; Figs. S3g; Borges et al., 2018; Crawford et al., 2016; Sanders et al., 2007). Crop stream CH_4 concentration was 390 nmol L^{-1} during base flow (Tab. 2), a concentration significantly lower (1,430 nmol L^{-1}) than chalk streams impacted by macrophyte vegetation in England (Sanders et al., 2007). This discrepancy probably resulted from the increased in silt and clay fraction during summer of the underlying sediment in chalk streams (Sanders et al., 2007). This would suggest that the permeability of chalk stream sediment became lower than that of sandy stream sediment and created stronger reducing conditions in chalk stream sediments, which likely increased the potential for methanogenesis (Baker et al., 1999; Findlay, 1995; Kankaala et al., 2005; Morrice et al., 1997). Sanders et al. (2007) also showed that the chalk streams' emissions of CH_4 to the atmosphere were approximately 50 times lower than the CH_4 production in stream sediments, illustrating the high potential for CH_4 oxidation

in the water column of crop stream. During base flow, a second explanation for higher CH_4 (and NH_4^+) concentrations in crop streams relative to forest streams could be differential hydrology. Drainage plot is a function of the water table height (hydraulic gradient, Darcy's law). During base flow, the water table in cropland was deeper than in forest (e.g., 4 m deeper in Sep. 2014; Fig. 2), and so during this period, potentially more forest groundwater was drained into crop streams. However, in forest streams we usually did not observe CH_4 (or NH_4^+) concentrations as high as in crop streams (Tab. 2; Fig. 7d) indicating that CH_4 (or NH_4^+) in crop streams primarily originated from crop stream sediments rather than from higher discharge of forest groundwater. In crop streams, CH_4 was correlated with NH_4^+ but not correlated with NO_3^- or DOC (Figs. 6d, 7c, d). Such relationships were also observed in the Meuse river basin (Belgium) (Borges et al., 2018) and in a global meta-analysis of riverine CH_4 (Stanley et al., 2016). In contrast, this does not fit the conceptual model of Schade et al (2016) developed from data in New Hampshire streams, whereby the CH_4 was positively correlated with DOC, while negatively related to NO_3^-.

Sandy sediments of low order stream beds impacted by eutrophication are significant areas of NO_3^- reduction over the spring and summer, lowering DOC and NO_3^- concentrations in stream water (Tab. 4; Figs. S3c, l; Böhlke et al., 2009; Mulholland et al., 2008; Sanders et al., 2007). Additionally, the decreased of stream velocity during base flow increased residence times of NO_3^- in the hyporheic zone and the time for denitrification (Bardini et al., 2012). In a small stream dominated by maize cropland in the USA, Böhlke et al. (2009) demonstrated that denitrification mainly occurred in sediments and not in the water column since integrated rates of pore-water denitrification derived from ^{15}N tracer profiles within the hyporheic zone were similar to the reach-scale rates derived from measurements in the stream. In crop streams, a portion of the NO_3^- variability between the two hydrological periods could also result from higher drainage of forest groundwater during base flow, which would dilute the NO_3^- signal from crop groundwater.

Considering the flat catchment topography, a minor portion of TSM and POC in streams originates from soil erosion and surface runoff. The most frequent effects of dredging on aquatic ecosystems are changes

592 in the concentration of suspended solids, turbidity and light penetration (Lewis et al., 2001; Newell et al.,
593 1998). Higher concentrations of POC (and TSM) observed in crop streams were also caused by
594 macrophyte biomass developed in summer became a sediment trap. When stream discharge was
595 sufficiently energetic, it re-suspended all the accumulated sediment and removed this litter. Moreover, we
596 observed peaks of CH_4 and NH_4^+ in crop streams during high flow (Tab. 4; Figs. S3d, g), suggesting that
597 dredging or streambed erosion of crop streams also release CH_4 and NH_4^+ from the sediment.

598 In forest streams, we observed significantly lower concentrations of Fe^{2+}, NH_4^+, and CH_4 than in forest
599 groundwater and significant negative linear relationships between O_2 on the one side and Fe^{2+}, NH_4^+, or
600 CH_4 (Tab. 2; Figs. 4d, e, g, 7e, f). This suggests there were low O_2 concentration groundwater inputs with
601 high concentrations of reduced compounds and that the stream water was gradually oxygenated, which
602 induced Fe^{2+} and CH_4 oxidations and nitrification. Mulholland et al. (2000) studied N cycling by adding
603 ^{15}N-labeled NH_4^+ into a forest stream in eastern Tennessee (USA). They concluded that the residence time
604 of NH_4^+ in the water column was low (5 min) and that nitrification was an important sink for NH_4^+,
605 accounting for 19% of total ammonium uptake. In forest streams, the NH_4^+ concentration was
606 approximately 3 µmol L^{-1} lower than in forest groundwater and thus did not explained the NO_3^- increase of
607 50 µmol L^{-1} (Tab. 2; Figs. 3c, d). Up to 76% of N exports from local forest are in organic forms but these
608 N exports are very low (< 0.2 g N m^{-2} yr^{-1}; De Wit et al., 2005; Rimmelin, 1998; Vernier et al., 2003), so
609 in-stream mineralization of organic N coupled to nitrification could not explain NO_3^- concentrations in
610 forest streams. Since the sampled forest streams are not strictly forested, NO_3^- concentration are explained
611 by simple hydrological mixing between crop and forest groundwater (Tab. 2).

612 In streams, pCO_2 was lower and O_2 was higher than in groundwater (Tab. 2; Figs. 3f, h, 5a). This shows
613 that gas exchange between stream water and the atmosphere occurs quickly, favored by low stream depth
614 and strong concentration gradients between the two compartments. Some authors (e.g., Bodmer et al.
615 2016; Borges et al., 2018) found elevated pCO_2 in crop streams rather than in forest streams, due to higher
616 levels of dissolved and particulate organic matter in crop dominated systems compared to the forested

617 ones that facilitated the in-stream degradation of organic matter. Moreover, land uses are expected to
618 change the composition of terrestrial soil organic matter leached to streams, shifting from vegetation- to
619 microbe-derived organic matter with greater agricultural land use and potentially higher emissions in crop
620 streams (Fuss et al., 2017; Graeber et al., 2015; Wilson and Xenopoulos, 2009). Those results contrasted
621 with ours because we found no difference in pCO_2 between crop and forest streams. Forest groundwater
622 did have higher pCO_2 than crop groundwater, indicating a more intense degassing in forest streams. The
623 similar δ^{13}C-DIC signatures in forest and crop streams despite the strong difference between crop and
624 forest groundwater suggests faster isotopic equilibration of DIC resulting from degassing. The greater gas
625 transfer velocity in forest streams is a consequence of the abundance of coarse woody debris which
626 generates higher levels of water turbulence (e.g., Bodmer et al. 2016), and is consistent with our field
627 observations. A lower gas transfer velocity lower in crop streams results from stream calibration reducing
628 turbulent flow, and macrophyte vegetation that protects the water surface from wind shear.

629

630 **5. Conclusion**

631 The present study demonstrates that C and IN concentrations in shallow groundwater and in first-order
632 streams are strongly sensitive to land use. In sandy lowland catchments, simultaneous measurements of
633 biogeochemical parameters in groundwater and streams are crucial for identifying and quantifying
634 biogeochemical processes involved at the groundwater-stream interface. We also show that a statistical
635 clustering analysis based on NO_3^- dataset enables partitioning of groundwater and streams into crop-
636 affected or forest-dominated waters. Such a classification could be useful to river managers and policy
637 makers. The water table had greater depth in croplands and was a crucial parameter necessary for
638 understanding groundwater biogeochemical variability in relation to land use. Higher water table stages in
639 forests created anoxic conditions and increased soil leaching. Conversely, in croplands, the deeper water
640 table prevented anoxic conditions, creating different groundwater compositions from forest groundwater
641 and inhibiting the denitrification of the N fertilizers, which led to groundwater NO_3^- accumulation. Despite

the occurrence of groundwater denitrification in riparian and forest sites, N fertilizers inputs in crop streams were still high enough to generate eutrophic conditions in these streams. Eutrophication resulted in a biogeochemical cascading effect, which sustained high CH_4 concentration and lowered NO_3^-. High CO_2 and CH_4 production occurs in forest soils and groundwater, but these two gases exhibit lower concentrations in forest streams, indicating intense degassing or oxidation.

The groundwater-stream interface is a biogeochemical hotspot and hot moment for C emissions and N removal processes (McClain et al., 2003). Future studies focusing on the groundwater-stream interface in relation to land use are needed to better understand C and N dynamics in aquatic systems in order to correctly close C and N budgets at regional and global scales.

Acknowledgments

This research is part of the CNP-Leyre project funded by the Cluster of Excellence COTE at the Université de Bordeaux (ANR-10-LABX-45).

Bibliography

Abril, G., Borges, A.V., 2018. Carbon leaks from flooded land: do we need to re-plumb the inland water active pipe? Biogeosciences Discuss. 2018, 1–46. https://doi.org/10.5194/bg-2018-239

Abril, G., Bouillon, S., Darchambeau, F., Teodoru, C.R., Marwick, T.R., Tamooh, F., Ochieng Omengo, F., Geeraert, N., Deirmendjian, L., Polsenaere, P., Borges, A.V., 2015. Technical Note: Large overestimation of pCO2 calculated from pH and alkalinity in acidic, organic-rich freshwaters. Biogeosciences 12, 67–78. https://doi.org/10.5194/bg-12-67-2015

Abril, G., Martinez, J.-M., Artigas, L.F., Moreira-Turcq, P., Benedetti, M.F., Vidal, L., Meziane, T., Kim, J.-H., Bernardes, M.C., Savoye, N., Deborde, J., Souza, E.L., Albéric, P., Landim de Souza, M.F., Roland, F., 2014. Amazon River carbon dioxide outgassing fuelled by wetlands. Nature 505, 395–398. https://doi.org/10.1038/nature12797

Aitkenhead, J.A., Hope, D., Billett, M.F., 1999. The relationship between dissolved organic carbon in stream water and soil organic carbon pools at different spatial scales. Hydrol. Process. 13, 1289–1302.

Anderson, L., 1979. Simultaneous spectrophotometric determination of nitrite and nitrate by flow injection analysis. Anal. Chim. Acta 110, 123–128.

672 Anderson, T.R., Groffman, P.M., Kaushal, S.S., Walter, M.T., 2014. Shallow groundwater denitrification in
673 riparian zones of a headwater agricultural landscape. J. Environ. Qual. 43, 732–744.
674 Asner, G.P., Elmore, A.J., Olander, L.P., Martin, R.E., Harris, A.T., 2004. Grazing systems, ecosystem
675 responses, and global change. Annu Rev Env. Resour 29, 261–299.
676 Augusto, L., Bakker, M.R., Morel, C., Meredieu, C., Trichet, P., Badeau, V., Arrouays, D., Plassard, C.,
677 Achat, D.L., Gallet-Budynek, A., Merzeau, D., Canteloup, D., Najar, M., Ranger, J., 2010. Is 'grey
678 literature' a reliable source of data to characterize soils at the scale of a region? A case study in a
679 maritime pine forest in southwestern France. Eur. J. Soil Sci. 61, 807–822.
680 https://doi.org/10.1111/j.1365-2389.2010.01286.x
681 Baker, M.A., Dahm, C.N., Valett, H.M., 1999. Acetate retention and metabolism in the hyporheic zone of
682 a mountain stream. Limnol. Oceanogr. 44, 1530–1539.
683 Bakker, M.R., Augusto, L., Achat, D.L., 2006. Fine root distribution of trees and understory in mature
684 stands of maritime pine (Pinus pinaster) on dry and humid sites. Plant Soil 286, 37–51.
685 Bakker, M.R., Jolicoeur, E., Trichet, P., Augusto, L., Plassard, C., Guinberteau, J., Loustau, D., 2009.
686 Adaptation of fine roots to annual fertilization and irrigation in a 13-year-old Pinus pinaster
687 stand. Tree Physiol. 29, 229–238.
688 Balestrini, R., Sacchi, E., Tidili, D., Delconte, C.A., Buffagni, A., 2016. Factors affecting agricultural nitrogen
689 removal in riparian strips: examples from groundwater-dependent ecosystems of the Po Valley
690 (Northern Italy). Agric. Ecosyst. Environ. 221, 132–144.
691 Barnes, R.T., Raymond, P.A., 2010. Land-use controls on sources and processing of nitrate in small
692 watersheds: insights from dual isotopic analysis. Ecol. Appl. 20, 1961–1978.
693 Barnes, R.T., Raymond, P.A., 2009. The contribution of agricultural and urban activities to inorganic
694 carbon fluxes within temperate watersheds. Chem. Geol. 266, 318–327.
695 Bass, A.M., Munksgaard, N.C., Leblanc, M., Tweed, S., Bird, M.I., 2014. Contrasting carbon export
696 dynamics of human impacted and pristine tropical catchments in response to a short-lived
697 discharge event. Hydrol. Process. 28, 1835–1843.
698 Bastviken, D., Tranvik, L.J., Downing, J.A., Crill, P.M., Enrich-Prast, A., 2011. Freshwater methane
699 emissions offset the continental carbon sink. Science 331, 50–50.
700 Bell, R.A., Darling, W.G., Ward, R.S., Basava-Reddi, L., Halwa, L., Manamsa, K., Dochartaigh, B.Ó., 2017. A
701 baseline survey of dissolved methane in aquifers of Great Britain. Sci. Total Environ. 601, 1803–
702 1813.
703 Bernot, M.J., Sobota, D.J., Hall, R.O., Mulholland, P.J., Dodds, W.K., Webster, J.R., Tank, J.L., Ashkenas,
704 L.R., Cooper, L.W., Dahm, C.N., 2010. Inter-regional comparison of land-use effects on stream
705 metabolism. Freshw. Biol. 55, 1874–1890.
706 Bertran, P., Allenet, G., Gé, T., Naughton, F., Poirier, P., Goñi, M.F.S., 2009. Coversand and Pleistocene
707 palaeosols in the Landes region, southwestern France. J. Quat. Sci. 24, 259–269.
708 Bertran, P., Bateman, M.D., Hernandez, M., Mercier, N., Millet, D., Sitzia, L., Tastet, J.-P., 2011. Inland
709 aeolian deposits of south-west France: facies, stratigraphy and chronology. J. Quat. Sci. 26, 374–
710 388.
711 Bodmer, P., Heinz, M., Pusch, M., Singer, G., Premke, K., 2016. Carbon dynamics and their link to
712 dissolved organic matter quality across contrasting stream ecosystems. Sci. Total Environ. 553,
713 574–586.
714 Böhlke, J.K., Antweiler, R.C., Harvey, J.W., Laursen, A.E., Smith, L.K., Smith, R.L., Voytek, M.A., 2009.
715 Multi-scale measurements and modeling of denitrification in streams with varying flow and
716 nitrate concentration in the upper Mississippi River basin, USA. Biogeochemistry 93, 117–141.
717 Borges, A.V., Darchambeau, F., Lambert, T., Bouillon, S., Morana, C., Brouyère, S., Hakoun, V., Jurado, A.,
718 Tseng, H.-C., Descy, J.-P., 2018. Effects of agricultural land use on fluvial carbon dioxide, methane

719 and nitrous oxide concentrations in a large European river, the Meuse (Belgium). Sci. Total
720 Environ. 610, 342–355.
721 Borges, A.V., Darchambeau, F., Teodoru, C.R., Marwick, T.R., Tamooh, F., Geeraert, N., Omengo, F.O.,
722 Guérin, F., Lambert, T., Morana, C., Okuku, E., Bouillon, S., 2015. Globally significant greenhouse-
723 gas emissions from African inland waters. Nat. Geosci. 8, 637–642.
724 https://doi.org/10.1038/ngeo2486
725 Camino-Serrano, M., Gielen, B., Luyssaert, S., Ciais, P., Vicca, S., Guenet, B., Vos, B.D., Cools, N., Ahrens,
726 B., Altaf Arain, M., Borken, W., Clarke, N., Clarkson, B., Cummins, T., Don, A., Graf Pannatier, E.,
727 Laudon, H., Moore, T., Nieminen, T.., Nilsson, M.B., Peichi, M., Schwendenmann, L., Siemens, J.,
728 Janssens, I.A., 2014. Linking variability in soil solution dissolved organic carbon to climate, soil
729 type, and vegetation type. Glob. Biogeochem. Cycles 28, 497–509.
730 https://doi.org/10.1002/2013GB004726.
731 Canton, M., Anschutz, P., Coynel, A., Polsenaere, P., Auby, I., Poirier, D., 2012. Nutrient export to an
732 Eastern Atlantic coastal zone: first modeling and nitrogen mass balance. Biogeochemistry 107,
733 361–377.
734 Carpenter, S.R., Caraco, N.F., Correll, D.L., Howarth, R.W., Sharpley, A.N., Smith, V.H., 1998. Nonpoint
735 pollution of surface waters with phosphorus and nitrogen. Ecol. Appl. 8, 559–568.
736 Cey, E.E., Rudolph, D.L., Aravena, R., Parkin, G., 1999. Role of the riparian zone in controlling the
737 distribution and fate of agricultural nitrogen near a small stream in southern Ontario. J. Contam.
738 Hydrol. 37, 45–67.
739 Christensen, J.R., Nash, M.S., Neale, A., 2013. Identifying riparian buffer effects on stream nitrogen in
740 southeastern coastal plain watersheds. Environ. Manage. 52, 1161–1176.
741 Christensen, T.R., Ekberg, A., Ström, L., Mastepanov, M., Panikov, N., Öquist, M., Svensson, B.H.,
742 Nykänen, H., Martikainen, P.J., Oskarsson, H., 2003. Factors controlling large scale variations in
743 methane emissions from wetlands. Geophys. Res. Lett. 30.
744 Ciais, P., Wattenbach, M., Vuichard, N., Smith, P., Piao, S.L., Don, A., Luyssaert, S., Janssens, I.A.,
745 Bondeau, A., Dechow, R., others, 2010. The European carbon balance. Part 2: croplands. Glob.
746 Change Biol. 16, 1409–1428.
747 Clague, J.C., Stenger, R., Clough, T.J., 2015. Denitrification in the shallow groundwater system of a
748 lowland catchment: a laboratory study. Catena 131, 109–118.
749 Clark, I., Fritz, P., 1997. Environmental isotopes in hydrology. Lewis Publishers, Boca Raton, Fla.
750 Cole, J.J., Prairie, Y.T., Caraco, N.F., McDowell, W.H., Tranvik, L.J., Striegl, R.G., Duarte, C.M., Kortelainen,
751 P., Downing, J.A., Middelburg, J.J., Melack, J., 2007. Plumbing the Global Carbon Cycle:
752 Integrating Inland Waters into the Terrestrial Carbon Budget. Ecosystems 10, 171–184.
753 https://doi.org/10.1007/s10021-006-9013-8
754 Corbier, P., Karnay, G., Bourgine, B., Saltel, M., 2010. Gestion des eaux souterraines en région Aquitaine -
755 Reconnaissance des potentialités aquifères du Mio-Plio-Quaternaire des kandes de Gascogne et
756 du Médoc en relation avec les SAGE, Module 7 (No. 57813). BRGM, Orléans, France.
757 Cotton, J.A., Wharton, G., Bass, J.A.B., Heppell, C.M., Wotton, R.S., 2006. The effects of seasonal changes
758 to in-stream vegetation cover on patterns of flow and accumulation of sediment.
759 Geomorphology 77, 320–334.
760 Crawford, J.T., Loken, L.C., Stanley, E.H., Stets, E.G., Dornblaser, M.M., Striegl, R.G., 2016. Basin scale
761 controls on CO2 and CH4 emissions from the Upper Mississippi River. Geophys. Res. Lett. 43,
762 1973–1979.
763 Das, A., Krishnaswami, S., Bhattacharya, S.K., 2005. Carbon isotope ratio of dissolved inorganic carbon
764 (DIC) in rivers draining the Deccan Traps, India: sources of DIC and their magnitudes. Earth
765 Planet. Sci. Lett. 236, 419–429.

766 Datry, T., Malard, F., Gibert, J., 2004. Dynamics of solutes and dissolved oxygen in shallow urban
767 groundwater below a stormwater infiltration basin. Sci. Total Environ. 329, 215–229.
768 De Carvalho, M.C., Hayashizaki, K.-I., Ogawa, H., 2009. SHORT-TERM MEASUREMENT OF CARBON STABLE
769 ISOTOPE DISCRIMINATION IN PHOTOSYNTHESIS AND RESPIRATION BY AQUATIC MACROPHYTES,
770 WITH MARINE MACROALGAL EXAMPLES 1. J. Phycol. 45, 761–770.
771 De Wit, R., Leibreich, J., Vernier, F., Delmas, F., Beuffe, H., Maison, P., Chossat, J.-C., Laplace-Treyture, C.,
772 Laplana, R., Clave, V., 2005. Relationship between land-use in the agro-forestry system of les
773 Landes, nitrogen loading to and risk of macro-algal blooming in the Bassin d'Arcachon coastal
774 lagoon (SW France). Estuar. Coast. Shelf Sci. 62, 453–465.
775 Deirmendjian, L., Abril, G., 2018. Carbon dioxide degassing at the groundwater-stream-atmosphere
776 interface: isotopic equilibration and hydrological mass balance in a sandy watershed. J. Hydrol.
777 558, 129–143. https://doi.org/10.1016/j.jhydrol.2018.01.003
778 Deirmendjian, L., Loustau, D., Augusto, L., Lafont, S., Chipeaux, C., Poirier, D., Abril, G., 2018. Hydro-
779 ecological controls on dissolved carbon dynamics in groundwater and export to streams in a
780 temperate pine forest. Biogeosciences 15, 669–691. https://doi.org/10.5194/bg-15-669-2018
781 Downing, J.A., Cole, J.J., Duarte, C.M., Middelburg, J.J., Melack, J.M., Prairie, Y.T., Kortelainen, P., Striegl,
782 R.G., McDowell, W.H., Tranvik, L.J., 2012. Global abundance and size distribution of streams and
783 rivers. Inland Waters 2, 229–236.
784 EEA, 2014. Corine Land Cover 2006 raster data. Eur. Environ. Agency EEA Available Httpwww Eea Eur.
785 Eudata--Mapsdatadsresolveuida645109f7a11d43f5d7e275d81f35c61 3.
786 Etcheber, H., Taillez, A., Abril, G., Garnier, J., Servais, P., Moatar, F., Commarieu, M.-V., 2007. Particulate
787 organic carbon in the estuarine turbidity maxima of the Gironde, Loire and Seine estuaries: origin
788 and lability. Hydrobiologia 588, 245–259.
789 Evans, S.D., Lindstrom, M.J., Voorhees, W.B., Moncrief, J.F., Nelson, G.A., 1996. Effect of subsoiling and
790 subsequent tillage on soil bulk density, soil moisture, and corn yield. Soil Tillage Res. 38, 35–46.
791 Findlay, S., 1995. Importance of surface-subsurface exchange in stream ecosystems: The hyporheic zone.
792 Limnol. Oceanogr. 40, 159–164.
793 Findlay, S., Quinn, J.M., Hickey, C.W., Burrell, G., Downes, M., 2001. Effects of land use and riparian
794 flowpath on delivery of dissolved organic carbon to streams. Limnol. Oceanogr. 46, 345–355.
795 Foley, J.A., DeFries, R., Asner, G.P., Barford, C., Bonan, G., Carpenter, S.R., Chapin, F.S., Coe, M.T., Daily,
796 G.C., Gibbs, H.K., 2005. Global consequences of land use. science 309, 570–574.
797 Foulquier, A., Malard, F., Mermillod-Blondin, F., Datry, T., Simon, L., Montuelle, B., Gibert, J., 2010.
798 Vertical change in dissolved organic carbon and oxygen at the water table region of an aquifer
799 recharged with stormwater: biological uptake or mixing? Biogeochemistry 99, 31–47.
800 Frankignoulle, M., Borges, A.V., 2001. Direct and Indirect pCO2 Measurements in a Wide Range of pCO2
801 and Salinity Values (The Scheldt Estuary). Aquat. Geochem. 7, 267–273.
802 https://doi.org/10.1023/A:1015251010481
803 Fuss, T., Behounek, B., Ulseth, A.J., Singer, G.A., 2017. Land use controls stream ecosystem metabolism
804 by shifting dissolved organic matter and nutrient regimes. Freshw. Biol. 62, 582–599.
805 Gillikin, D.P., Bouillon, S., 2007. Determination of δ18O of water and δ13C of dissolved inorganic carbon
806 using a simple modification of an elemental analyser-isotope ratio mass spectrometer: an
807 evaluation. Rapid Commun. Mass Spectrom. 21, 1475–1478.
808 Gleick, P.H., 2003. Water use. Annu. Rev. Environ. Resour. 28, 275–314.
809 Goldscheider, N., Hunkeler, D., Rossi, P., 2006. Microbial biocenoses in pristine aquifers and an
810 assessment of investigative methods. Hydrogeol. J. 14, 926–941.
811 Govind, A., Bonnefond, J.-M., Kumari, J., Moisy, C., Loustau, D., Wigneron, J.-P., 2012. Modeling the
812 ecohydrological processes in the Landes de Gascogne, SW France, in: Plant Growth Modeling,

Simulation, Visualization and Applications (PMA), 2012 IEEE Fourth International Symposium On. IEEE, pp. 133–140.
Graeber, D., Boëchat, I.G., Encina-Montoya, F., Esse, C., Gelbrecht, J., Goyenola, G., Gücker, B., Heinz, M., Kronvang, B., Meerhoff, M., 2015. Global effects of agriculture on fluvial dissolved organic matter. Sci. Rep. 5.
Gran, G., 1952. Determination of the equivalence point in potentiometric titrations of seawater with hydrochloric acid. Ocean. Acta 5, 209–218.
Hagedorn, F., Kaiser, K., Feyen, H., Schleppi, P., 2000. Effects of redox conditions and flow processes on the mobility of dissolved organic carbon and nitrogen in a forest soil. J. Environ. Qual. 29, 288–297.
Hagerdon, F., Schleppi, P., Waldner, P., Fluhler, H., 2000. Export of dissolved organic carbon and nitrogen from Gleysol dominated catchments–the significance of water flow paths. Biogeochemistry 50, 137–161.
Harwood, J.E., Kühn, A.L., 1970. A colorimetric method for ammonia in natural waters. Water Res. 4, 805–811. https://doi.org/10.1016/0043-1354(70)90037-0
Hiscock, K.M., Lloyd, J.W., Lerner, D.N., 1991. Review of natural and artificial denitrification of groundwater. Water Res. 25, 1099–1111.
Hotchkiss, E.R., Hall Jr, R.O., Sponseller, R.A., Butman, D., Klaminder, J., Laudon, H., Rosvall, M., Karlsson, J., 2015. Sources of and processes controlling CO2 emissions change with the size of streams and rivers. Nat. Geosci. 8, 696–699.
Hu, Y., Lu, Y., Edmonds, J.W., Liu, C., Wang, S., Das, O., Liu, J., Zheng, C., 2016. Hydrological and land use control of watershed exports of dissolved organic matter in a large arid river basin in northwestern China. J. Geophys. Res. Biogeosciences 121, 466–478.
Jackson, R.B., Carpenter, S.R., Dahm, C.N., McKnight, D.M., Naiman, R.J., Postel, S.L., Running, S.W., 2001. Water in a changing world. Ecol. Appl. 11, 1027–1045.
Jambert, C., Delmas, R.A., Labroue, L., Chassin, P., 1994. Nitrogen compound emissions from fertilized soils in a maize field pine tree forest agrosystem in the southwest of France. J. Geophys. Res. Atmospheres 99, 16523–16530.
Jambert, C., Serca, D., Delmas, R., 1997. Quantification of N-losses as NH 3, NO, and N 2 O and N 2 from fertilized maize fields in southwestern France. Nutr. Cycl. Agroecosystems 48, 91–104.
Jeong, C.H., 2001. Effect of land use and urbanization on hydrochemistry and contamination of groundwater from Taejon area, Korea. J. Hydrol. 253, 194–210.
Johnson, M.S., Lehmann, J., Couto, E.G., Novaes Filho, J.P., Riha, S.J., 2006. DOC and DIC in flowpaths of Amazonian headwater catchments with hydrologically contrasting soils. Biogeochemistry 81, 45–57.
Johnson, M.S., Lehmann, J., Riha, S.J., Krusche, A.V., Richey, J.E., Ometto, J.P.H., Couto, E.G., 2008. CO2 efflux from Amazonian headwater streams represents a significant fate for deep soil respiration. Geophys. Res. Lett. 35, L17401. https://doi.org/10.1029/2008GL034619.
Jolivet, C., Arrouays, D., Andreux, F., Lévèque, J., 1997. Soil organic carbon dynamics in cleared temperate forest spodosols converted to maize cropping. Plant Soil 191, 225–231.
Jolivet, C., Arrouays, D., Leveque, J., Andreux, F., Chenu, C., 2003. Organic carbon dynamics in soil particle-size separates of sandy Spodosols when forest is cleared for maize cropping. Eur. J. Soil Sci. 54, 257–268.
Jolivet, C., Augusto, L., Trichet, P., Arrouays, D., 2007. Forest soils in the Gascony Landes Region: formation, history, properties and spatial varaibility. Rev. For. Fr. 59, 7–30. https://doi.org/10.4267/2042/8480
Jones, J.B., Mulholland, P.J., 1998. Carbon dioxide variation in a hardwood forest stream: an integrative measure of whole catchment soil respiration. Ecosystems 1, 183–196.

Jordan, T.E., Weller, D.E., 1996. Human contributions to terrestrial nitrogen flux. BioScience 46, 655–664.
Jurado, A., Borges, A., Pujades, E., Hakoun, V., Knöller, K., Brouyère, S., 2017. Occurrence of greenhouse gases (CO2, N2O and CH4) in groundwater of the Walloon Region (Belgium).
Juste, C., Tauzin, J., Dureau, P., Courpron, C., 1982. Exportation des éléments fertilisants par lessivage en sol sableux des Landes de Gascogne. Résultats de 8 années d'observations en cases lysimétriques. Agronomie 2, 91–98.
Kankaala, P., Käki, T., Mäkelä, S., Ojala, A., Pajunen, H., Arvola, L., 2005. Methane efflux in relation to plant biomass and sediment characteristics in stands of three common emergent macrophytes in boreal mesoeutrophic lakes. Glob. Change Biol. 11, 145–153.
Kassambra, A., Mundt, F., 2017. factoextra: Extract and Visualize the Results of Multivariate Data Analyses. R package version 1.0.5.
Klüber, H.D., Conrad, R., 1998. Effects of nitrate, nitrite, NO and N2O on methanogenesis and other redox processes in anoxic rice field soil. FEMS Microbiol. Ecol. 25, 301–318.
Kokic, J., Wallin, M.B., Chmiel, H.E., Denfeld, B.A., Sobek, S., 2015. Carbon dioxide evasion from headwater systems strongly contributes to the total export of carbon from a small boreal lake catchment. J. Geophys. Res. Biogeosciences 120, 13–28. https://doi.org/10.1002/2014JG002706
Kolbjørn Jensen, J., Engesgaard, P., Johnsen, A.R., Marti, V., Nilsson, B., 2017. Hydrological mediated denitrification in groundwater below a seasonal flooded restored riparian zone. Water Resour. Res. 53, 2074–2094.
Korom, S.F., 1992. Natural denitrification in the saturated zone: a review. Water Resour. Res. 28, 1657–1668.
Lamba, J., Thompson, A.M., Karthikeyan, Kg., Fitzpatrick, F.A., 2015. Sources of fine sediment stored in agricultural lowland streams, Midwest, USA. Geomorphology 236, 44–53.
Lauerwald, R., Laruelle, G.G., Hartmann, J., Ciais, P., Regnier, P.A., 2015. Spatial patterns in CO2 evasion from the global river network. Glob. Biogeochem. Cycles 29, 534–554.
Lê, S., Josse, J., Husson, F., 2008. FactoMineR: an R package for multivariate analysis. J. Stat. Softw. 25, 1–18.
Legigan, P., 1979. L'élaboration de la formation du sable des Landes, dépôt résiduel de l'environnement sédimentaire pliocène-pléïstocène centre aquitain (Thèse de Doctorat d'Etat n°642). Université de Bordeaux I, Bordeaux.
Lehrter, J.C., 2006. Effects of land use and land cover, stream discharge, and interannual climate on the magnitude and timing of nitrogen, phosphorus, and organic carbon concentrations in three coastal plain watersheds. Water Environ. Res. 78, 2356–2368.
Lewis, E., Wallace, D., Allison, L.J., 1998. Program developed for CO2 system calculations. Carbon Dioxide Information Analysis Center, managed by Lockheed Martin Energy Research Corporation for the US Department of Energy Tennessee, Oak Ridge, Tennessee.
Lewis, M.A., Weber, D.E., Stanley, R.S., Moore, J.C., 2001. Dredging impact on an urbanized Florida bayou: effects on benthos and algal-periphyton. Environ. Pollut. 115, 161–171.
Ludwig, W., Amiotte-Suchet, P., Probst, J.-L., 1996a. River discharges of carbon to the world's oceans: determining local inputs of alkalinity and of dissolved and particulate organic carbon. Sci. Terre Planètes Comptes Rendus Académie Sci. 323, 1007–1014.
Ludwig, W., Probst, J.-L., Kempe, S., 1996b. Predicting the oceanic input of organic carbon by continental erosion. Glob. Biogeochem. Cycles 10, 23–41.
Lundström, U.S., van Breemen, N., Bain, D., 2000. The podzolization process. A review. Geoderma 94, 91–107.
MacQueen, J., 1967. Some methods for classification and analysis of multivariate observations, in: Proceedings of the Fifth Berkeley Symposium on Mathematical Statistics and Probability. Oakland, CA, USA, pp. 281–297.

Malard, F., Hervant, F., 1999. Oxygen supply and the adaptations of animals in groundwater. Freshw. Biol. 41, 1–30.
Marx, A., Dusek, J., Jankovec, J., Sanda, M., Vogel, T., Geldern, R., Hartmann, J., Barth, J.A.C., 2017. A review of CO2 and associated carbon dynamics in headwater streams: a global perspective. Rev. Geophys.
Masese, F.O., Salcedo-Borda, J.S., Gettel, G.M., Irvine, K., McClain, M.E., 2017. Influence of catchment land use and seasonality on dissolved organic matter composition and ecosystem metabolism in headwater streams of a Kenyan river. Biogeochemistry 132, 1–22.
McAleer, E.B., Coxon, C.E., Richards, K.G., Jahangir, M.M.R., Grant, J., Mellander, P.E., 2017. Groundwater nitrate reduction versus dissolved gas production: a tale of two catchments. Sci. Total Environ. 586, 372–389.
McClain, M.E., Boyer, E.W., Dent, C.L., Gergel, S.E., Grimm, N.B., Groffman, P.M., Hart, S.C., Harvey, J.W., Johnston, C.A., Mayorga, E., McDowell, W.H., Pinay, G., 2003. Biogeochemical hot spots and hot moments at the interface of terrestrial and aquatic ecosystems. Ecosystems 6, 301–312.
McMahon, P.B., Chapelle, F.H., 2008. Redox processes and water quality of selected principal aquifer systems. Groundwater 46, 259–271.
Mekala, C., Gaonkar, O., Nambi, I.M., 2017. Understanding nitrogen and carbon biogeotransformations and transport dynamics in saturated soil columns. Geoderma 285, 185–194.
Meybeck, M., 1987. Global chemical weathering of surficial rocks estimated from river dissolved loads. Am. J. Sci. 401–428.
Meybeck, M., 1982. Carbon, nitrogen, and phosphorus transport by world rivers. Am J Sci 282, 401–450.
Millero, F.J., 1979. The thermodynamics of the carbonate system in seawater. Geochim. Cosmochim. Acta 43, 1651–1661.
Molofsky, L.J., Connor, J.A., McHugh, T.E., Richardson, S.D., Woroszylo, C., Alvarez, P.J., 2016. Environmental factors associated with natural methane occurrence in the Appalachian Basin. Groundwater 54, 656–668.
Montgomery, D.R., 2007. Soil erosion and agricultural sustainability. Proc. Natl. Acad. Sci. 104, 13268–13272.
Moore, T.R., Knowles, R., 1989. The influence of water table levels on methane and carbon dioxide emissions from peatland soils. Can. J. Soil Sci. 69, 33–38.
Moreaux, V., Lamaud, É., Bosc, A., Bonnefond, J.-M., Medlyn, B.E., Loustau, D., 2011. Paired comparison of water, energy and carbon exchanges over two young maritime pine stands (Pinus pinaster Ait.): effects of thinning and weeding in the early stage of tree growth. Tree Physiol. 903–921. https://doi.org/10.1093/treephys/tpr048
Morrice, J.A., Valett, H.M., Dahm, C.N., Campana, M.E., 1997. Alluvial characteristics, groundwater–surface water exchange and hydrological retention in headwater streams. Hydrol. Process. 11, 253–267.
Mulholland, P.J., Helton, A.M., Poole, G.C., Hall, R.O., Hamilton, S.K., Peterson, B.J., Tank, J.L., Ashkenas, L.R., Cooper, L.W., Dahm, C.N., 2008. Stream denitrification across biomes and its response to anthropogenic nitrate loading. Nature 452, 202.
Mulholland, P.J., Tank, J.L., Sanzone, D.M., Wollheim, W.M., Peterson, B.J., Webster, J.R., Meyer, J.L., 2000. Nitrogen cycling in a forest stream determined by a 15N tracer addition. Ecol. Monogr. 70, 471–493.
Naumburg, E., Mata-Gonzalez, R., Hunter, R.G., Mclendon, T., Martin, D.W., 2005. Phreatophytic vegetation and groundwater fluctuations: a review of current research and application of ecosystem response modeling with an emphasis on Great Basin vegetation. Environ. Manage. 35, 726–740.

Newell, R.C., Seiderer, L.J., Hitchcock, D.R., 1998. The impact of dredging works in coastal waters: a review of the sensitivity to disturbance and subsequent recovery of biological resources on the sea bed. Oceanogr. Mar. Biol. Annu. Rev. 36, 127–178.

O'Leary, M.H., 1988. Carbon isotopes in photosynthesis. Bioscience 328–336.

Onderka, M., Pekarova, P., Miklanek, P., Halmova, D., Pekar, J., 2010. Examination of the dissolved inorganic nitrogen budget in three experimental microbasins with contrasting land cover—a mass balance approach. Water. Air. Soil Pollut. 210, 221–230.

O'Reilly, A.M., Chang, N.-B., Wanielista, M.P., 2012. Cyclic biogeochemical processes and nitrogen fate beneath a subtropical stormwater infiltration basin. J. Contam. Hydrol. 133, 53–75.

Otero, N., Torrentó, C., Soler, A., Menció, A., Mas-Pla, J., 2009. Monitoring groundwater nitrate attenuation in a regional system coupling hydrogeology with multi-isotopic methods: the case of Plana de Vic (Osona, Spain). Agric. Ecosyst. Environ. 133, 103–113.

Pabich, W.J., Valiela, I., Hemond, H.F., 2001. Relationship between DOC concentration and vadose zone thickness and depth below water table in groundwater of Cape Cod, USA. Biogeochemistry 55, 247–268.

Polsenaere, P., Abril, G., 2012. Modelling CO2 degassing from small acidic rivers using water pCO2, DIC and δ13C-DIC data. Geochim. Cosmochim. Acta 91, 220–239. https://doi.org/10.1016/j.gca.2012.05.030

Polsenaere, P., Savoye, N., Etcheber, H., Canton, M., Poirier, D., Bouillon, S., Abril, G., 2013. Export and degassing of terrestrial carbon through watercourses draining a temperate podzolized catchment. Aquat. Sci. 75, 299–319.

Postel, S., 1999. Pillar of sand: can the irrigation miracle last? WW Norton & Company.

Quénéa, K., Derenne, S., Largeau, C., Rumpel, C., Mariotti, A., 2006. Influence of change in land use on the refractory organic macromolecular fraction of a sandy spodosol (Landes de Gascogne, France). Geoderma 136, 136–151.

Quinton, J.N., Govers, G., Van Oost, K., Bardgett, R.D., 2010. The impact of agricultural soil erosion on biogeochemical cycling. Nat. Geosci. 3, 311–314.

R Core Team, 2018. R: A language and environment for statistical computing. R Foundation for Statistical Computing, Vienna, Austria.

Ramankutty, N., Foley, J.A., 1999. Estimating historical changes in global land cover: Croplands from 1700 to 1992. Glob. Biogeochem. Cycles 13, 997–1027.

Ramos, T.B., Rodrigues, S., Branco, M.A., Prazeres, A., Brito, D., Gonçalves, M.C., Martins, J.C., Fernandes, M.L., Pires, F.P., 2015. Temporal variability of soil organic carbon transport in the Enxoé agricultural watershed. Environ. Earth Sci. 73, 6663–6676.

Raven, J.A., Johnston, A.M., Kübler, J.E., Korb, R., McInroy, S.G., Handley, L.L., Scrimgeour, C.M., Walker, D.I., Beardall, J., Vanderklift, M., 2002. Mechanistic interpretation of carbon isotope discrimination by marine macroalgae and seagrasses. Funct. Plant Biol. 29, 355–378.

Ravishankara, A.R., Daniel, J.S., Portmann, R.W., 2009. Nitrous oxide (N2O): the dominant ozone-depleting substance emitted in the 21st century. science 326, 123–125.

Raymond, P.A., Cole, J.J., 2003. Increase in the export of alkalinity from North America's largest river. Science 301, 88–91.

Raymond, P.A., Hartmann, J., Lauerwald, R., Sobek, S., McDonald, C., Hoover, M., Butman, D., Striegl, R., Mayorga, E., Humborg, C., Kortelainen, P., Dürr, H., Meybeck, M., Ciais, P., Guth, P., 2013. Global carbon dioxide emissions from inland waters. Nature 503, 355–359. https://doi.org/10.1038/nature12760

Rimmelin, P., 1998. Etude des apports allochtones d'azote inorganique dissous parvenant à un système lagunaire: le Bassin d'Arcachon.

1003 Robinson, M., Ryder, E.L., Ward, R.C., 1985. Influence on streamflow of field drainage in a small
1004 agricultural catchment. Agric. Water Manag. 10, 145–158.
1005 Rodrigues, V., Estrany, J., Ranzini, M., de Cicco, V., Martín-Benito, J.M.T., Hedo, J., Lucas-Borja, M.E.,
1006 2018. Effects of land use and seasonality on stream water quality in a small tropical catchment:
1007 The headwater of Córrego Água Limpa, São Paulo (Brazil). Sci. Total Environ. 622, 1553–1561.
1008 Rosegrant, M.W., Cai, X., Cline, S.A., 2002. World water and food to 2025: dealing with scarcity. Intl Food
1009 Policy Res Inst.
1010 Rubol, S., Dutta, T., Rocchini, D., 2016. 2D visualization captures the local heterogeneity of oxidative
1011 metabolism across soils from diverse land-use. Sci. Total Environ. 572, 713–723.
1012 Rubol, S., Silver, W.L., Bellin, A., 2012. Hydrologic control on redox and nitrogen dynamics in a peatland
1013 soil. Sci. Total Environ. 432, 37–46.
1014 Salomons, W., Mook, W.G., 1986. Isotope geochemistry of carbonates in the weathering zone. Handb.
1015 Environ. Isot. Geochem. 2, 239–269.
1016 Salvia-Castellví, M., Iffly, J.F., Vander Borght, P., Hoffmann, L., 2005. Dissolved and particulate nutrient
1017 export from rural catchments: a case study from Luxembourg. Sci. Total Environ. 344, 51–65.
1018 Sanders, I.A., Heppell, C.M., Cotton, J.A., Wharton, G., Hildrew, A.G., Flowers, E.J., Trimmer, M., 2007.
1019 Emission of methane from chalk streams has potential implications for agricultural practices.
1020 Freshw. Biol. 52, 1176–1186.
1021 Sand-Jensen, K., Pedersen, O., 1999. Velocity gradients and turbulence around macrophyte stands in
1022 streams. Freshw. Biol. 42, 315–328.
1023 Schade, J.D., Bailio, J., McDowell, W.H., 2016. Greenhouse gas flux from headwater streams in New
1024 Hampshire, USA: Patterns and drivers. Limnol. Oceanogr. 61.
1025 Sharp, J.H., 1993. The dissolved organic carbon controversy: an update. Oceanography 6.
1026 Silver, W.L., Lugo, A.E., Keller, M., 1999. Soil oxygen availability and biogeochemistry along rainfall and
1027 topographic gradients in upland wet tropical forest soils. Biogeochemistry 44, 301–328.
1028 Smith, V.H., 2003. Eutrophication of freshwater and coastal marine ecosystems a global problem.
1029 Environ. Sci. Pollut. Res. 10, 126–139.
1030 Stanley, E.H., Casson, N.J., Christel, S.T., Crawford, J.T., Loken, L.C., Oliver, S.K., 2016. The ecology of
1031 methane in streams and rivers: patterns, controls, and global significance. Ecol. Monogr. 86,
1032 146–171.
1033 Starr, R.C., Gillham, R.W., 1993. Denitrification and organic carbon availability in two aquifers.
1034 Groundwater 31, 934–947.
1035 Stella, P., Lamaud, E., Brunet, Y., Bonnefond, J.-M., Loustau, D., Irvine, M., 2009. Simultaneous
1036 measurements of CO 2 and water exchanges over three agroecosystems in South-West France.
1037 Biogeosciences 6, 2957–2971.
1038 Stookey, L.L., 1970. Ferrozine—a new spectrophotometric reagent for iron. Anal. Chem. 42, 779–781.
1039 Stott, T., 2005. Natural recovery from accelerated forest ditch and stream bank erosion five years after
1040 harvesting of plantation forest on Plynlimon, mid-Wales. Earth Surf. Process. Landf. J. Br.
1041 Geomorphol. Res. Group 30, 349–357.
1042 Thivolle-Cazat, A., Najar, M., 2001. Évolution de la productivité et de la récolte du pin maritime dans le
1043 massif Landais. Evaluation de la disponibilité future en Gironde. Rev. For. Fr. 53, 351–355.
1044 Trichet, P., Bakker, M.R., Augusto, L., Alazard, P., Merzeau, D., Saur, E., 2009. Fifty years of fertilization
1045 experiments on Pinus pinaster in Southwest France: the importance of phosphorus as a fertilizer.
1046 For. Sci. 55, 390–402.
1047 Tsypin, M., Macpherson, G.L., 2012. The effect of precipitation events on inorganic carbon in soil and
1048 shallow groundwater, Konza Prairie LTER Site, NE Kansas, USA. Appl. Geochem. 27, 2356–2369.

Ulrich, E., Coddeville, P., Lanier, M., 2002. Retombées atmosphériques humides en France entre 1993 et 1998:[données et références-coordination technique de la surveillance de la qualité de l'air]. Ademe.
Vernier, F., Beuffe, H., Chossat, J.-C., 2003. Forêt et ressource en eau: étude de deux bassins versants en sol sableux (Landes de Gascogne). Rev. For. Fr. 55, 523–542.
Vernier, F., Castro, A., 2010. Critère Préservation de l'environnement Sous-critère Eau (Rapport d'expertise: Critère "Préservation de l'environnement"). GIP-ECOFOR, Bordeaux, France.
Vidon, P., Wagner, L.E., Soyeux, E., 2008. Changes in the character of DOC in streams during storms in two Midwestern watersheds with contrasting land uses. Biogeochemistry 88, 257–270.
Vogel, J.C., Ehleringer, J.R., Hall, A.E., Farquhar, G.D., 1993. Variability of carbon isotope fractionation during photosynthesis., in: Stable Isotopes and Plant Carbon-Water Relations. Academic Press Inc., pp. 29–46.
Wachniew, P., 2006. Isotopic composition of dissolved inorganic carbon in a large polluted river: The Vistula, Poland. Chem. Geol. 233, 293–308.
Wallin, M.B., Grabs, T., Buffam, I., Laudon, H., Ågren, A., Öquist, M.G., Bishop, K., 2013. Evasion of CO2 from streams – The dominant component of the carbon export through the aquatic conduit in a boreal landscape. Glob. Change Biol. 19, 785–797. https://doi.org/10.1111/gcb.12083
Weiss, R., 1974. Carbon dioxide in water and seawater: the solubility of a non-ideal gas. Mar. Chem. 2, 203–215.
Widdel, F., Schnell, S., Heising, S., Ehrenreich, A., Assmus, B., Schink, B., 1993. Ferrous iron oxidation by anoxygenic phototrophic bacteria. Nature 362, 834.
Wilson, H.F., Xenopoulos, M.A., 2009. Effects of agricultural land use on the composition of fluvial dissolved organic matter. Nat. Geosci. 2, 37–41.
Wynn, T.M., Mostaghimi, S., 2006. Effects of riparian vegetation on stream bank subaerial processes in southwestern Virginia, USA. Earth Surf. Process. Landf. J. Br. Geomorphol. Res. Group 31, 399–413.
Young, R.G., Huryn, A.D., 1999. Effects of land use on stream metabolism and organic matter turnover. Ecol. Appl. 9, 1359–1376.
Zhang, F., Wang, J., Wang, X., 2018. Recognizing the Relationship between Spatial Patterns in Water Quality and Land-Use/Cover Types: A Case Study of the Jinghe Oasis in Xinjiang, China. Water 10, 646.
Zhou, Y., Xu, J.F., Yin, W., Ai, L., Fang, N.F., Tan, W.F., Yan, F.L., Shi, Z.H., 2017. Hydrological and environmental controls of the stream nitrate concentration and flux in a small agricultural watershed. J. Hydrol. 545, 355–366.

Stream Order	Description	Catchment area (km²)[a]	Crop (%)[b]	Forest (%)[b]	Urban (%)[b]	During High Flow[c]	During Base Flow[c]
1	Ditch	1.0	86.5	13.5	0.0	C	C
1	Ditch	1.3	53.8	46.2	0.0	C	C
1	Ditch	11.3	44.2	55.8	0.0	C	C
1	Ditch	13.4	42.5	57.5	0.0	C	C
1	Stream	57.0	30.7	69.3	0.0	C	C
1	Stream	16.8	7.8	92.2	0.0	F	F
1	Ditch	7.9	5.8	94.2	0.0	F	F
1	Ditch	2.3	5.2	94.8	0.0	F	C
1	Stream	16.0	4.6	93.8	1.6	C	F
1	Stream	34.0	3.8	96.2	0.0	F	F
1	Stream	31.0	2.3	97.7	0.0	F	F
1	Headwater	0.3	0.0	100.0	0.0	F	F
0	Groundwater in a riparian forest but very near (5m) a maize cropland (P1)					R	R
0	Groundwater in maize cropland (P2)					C	C
0	Groundwater in maize cropland (P3)					C	C
0	Groundwater in pine forest (P4)					F	F
0	Groundwater in pine forest (P5)					F	F

Table 1. Characteristics of groundwater and stream sampling stations, ranked in decreasing order of cropland percentage in their respective sub-catchments. [a] delimited with a geographic information system software (ArcGIS 10.5®) using an hydrological database in a polyline form (BD CARTHAGE®) and a digital elevation model (BD ALTI®, resolution of 25m), which both have been made available by the national geographic institute of France (http://www.ign.fr/). [b] retrieved with the CORINE land cover 2006 database (EEA, 2014) using a geographic information system software (ArcGIS 10.5®). [c] C, F, R corresponding to crop, forest and riparian waters, respectively, either during high or base flow. Piezometer 1 (P1) is located in a riparian mixed pine and oak forest near a first-order stream and near a maize cropland, which where P2 is located. P2 and P3 are located in the middle of two different maize croplands of 0.6 km² and 6 km², respectively. P5 is located in an 11-years old pine plot of 0.6 km² and is part of the ICOS (name is FR-Bil) research infrastructure (http://icos-ri.eu), whereas P4 is located in another pine forest (approximately same age as P5 pine forest). The depth of piezometers (from the soil surface to the bottom of the piezometer) is 5.3m for P1, 4.9m for P2, 9.1m for P3, 5m for P4 and P5.

1097

	Crop continuum		Forest continuum		Riparian groundwater
	Groundwaters (22)	Streams (59)	Groundwaters (22)	Streams (78)	Groundwaters (11)
pH	4.5±0.2	6.0±0.3	4.5±0.3	5.8±0.5	4.7±0.1
	4.3-5.0	5.4-7.0	3.7-4.8	4.2-6.9	4.4-4.8
Temperature (°C)	14.5±1.8	13.6±4.2	12.8±1.8	12.9±3.9	14.9±2.4
	10.7-17.5	6.4-25.8	8.5-15.1	4.8-22.1	11.8-17.9
EC ($\mu S\ cm^{-1}$)	360±70	220±55	90±10	115±30	160±50
	220-465	75-370	65-115	70-200	95-270
NO_3^- ($\mu mol\ L^{-1}$)	1,140±485	340±200	25±40	75±70	310±260
	260-1,785	10-950	0-120	0-275	40-860
NH_4^+ ($\mu mol\ L^{-1}$)	0.4±0.8	6.1±7.0	4.5±7.0	1.8±1.7	0.4±0.4
	0-3.5	0-40	0.3-30	0-7.8	0-1.5
Fe^{2+} ($\mu mol\ L^{-1}$)	0.9±0.4	5.9±4.4	15±15	7.9±12.0	0.6±0.5
	0.1-1.9	0.1-22	0.9±56	0.6±58	0.2-1.5
O_2 ($\mu mol\ L^{-1}$)	220±65	290+45	20±30	280±50	100±70
	100-315	160-400	0-110	110-370	0-170
CH_4 ($nmol\ L^{-1}$)	40±25	460±950	1,770±1,830	240±300	1,470±1,490
	15-130	20-4,900	50-6,700	20-2,370	30-4,150
pCO_2 (ppmv)	30,650±11,590	4,480±2,680	50,630±26,070	4,900±4,500	42,950±28,560
	19,000-60,550	1,040-14,080	7,680-116,380	1,000-27,200	17,300-103,300
TA ($\mu mol\ L^{-1}$)	90±25	100±50	70±30	90±50	70±15
	35-130	30-300	30-135	30-280	45-85
δ^{13}C-DIC (‰)	-19.8±1.3	-18.2±3.5	-26.7±1.0	-19.8±2.8	-25.2±1.1
	-22 to -17.6	-27.6 to -11.3	-28.8 to -24	-27.6 to -14	-27.9 to -23.4
DIC ($\mu mol\ L^{-1}$)	1,450±480	315±135	2,460±1,130	320±210	1,960±1,150
	820-2,590	90-650	570-5,370	120-1,280	940-4,480
DOC ($\mu mol\ L^{-1}$)	510±150	605±320	930±930	470±250	400±100
	275-880	220-2,290	310-3,670	190-1,725	280-620
TSM ($mg\ L^{-1}$)		5.6±8.6		2.3±1.7	
		0.1-50.5		0.4-8.2	
POC (%)		28±10		28±10	
		0-50		10-80	
POC ($\mu mol\ L^{-1}$)		120±180		50±35	
		0-1,100		0-170	

1098 Tab. 2. Values of carbon and ancillary parameters throughout sampling period (Jan. 2014-Jul. 2015) in crop and forest continuums and in riparian
1099 groundwater. Numbers between brackets are corresponding to the sampling size. For each parameter, the table showed average±standard
1100 deviations and the range.

	Groundwater					
	Cropland_HF (4)	Cropland_BF (18)	Forest_HF (6)	Forest_BF (16)	Riparian_HF (2)	Riparian_BF (9)
pH	4.6±0.3	4.5±0.2	4.4±0.3	4.5±0.3	4.7±0.1	4.6±0.1
	4.3-4.9	4.3-5.0	4.0-4.8	3.7-4.8	4.6-4.8	4.4-4.8
Temperature (°C)	12.8±1.7	14.9±1.6	10.8±1.4	13.5±1.4	12.2±0.6	15.6±2.2
	10.7-14.5	11.6-17.5	8.5-12.2	10.7-15.1	11.8-12.6	12.1-17.9
EC ($\mu S\ cm^{-1}$)	370±60	360±70	90±15	90±10	200±20	150±50
	320-460	220-470	70-115	70-115	185-215	95-270
NO_3^- ($\mu mol\ L^{-1}$)	1,040±300	1,160±420	30±50	20±40	510±20	260±270
	760-1,320	260-1785	0-120	0-120	500-520	40-860
NH_4^+ ($\mu mol\ L^{-1}$)	0.5±0.4	0.4±0.9	3.3±2.2	5.0±8.0	0.3±0.1	0.4±0.5
	0.1-1	0-3.5	1.1-7	0-3-30	0.2-0.3	0-1.5
Fe^{2+} ($\mu mol\ L^{-1}$)	0.8±0.2	0.9±0.4	10.0±8.2	15±15	0.4±0.2	0.7±0.5
	0.7-1.1	0.1-1.9	2.7-25.5	0.9-56.6	0.2-0.5	0.2-1.5
O_2 ($\mu mol\ L^{-1}$)	250±90	220±70	20±20	20±30	170±0	100±80
	180-310	100-320	0-40	0-110	170-170	0-200
CH_4 ($nmol\ L^{-1}$)	30±3	50±25	480±630	2,260±1,900	1,460±2,010	1,470±1,500
	25-30	16-130	50-1,700	50-6,700	40-2,880	30-4,150
pCO_2 (ppmv)	22,050±2,000	32,560±12,000	28,100±11,580	59,080±25,060	21,530±5,950	47,700±29,590
	19,800-24,270	19,000-60,550	7,680-39,000	29,685-116,400	17,320-25,740	20,600-103,300
TA ($\mu mol\ L^{-1}$)	85±2	92±30	95±40	65±30	83±2	60-10
	82-86	35-130	60-135	30-100	82-85	45-75
$\delta^{13}C$-DIC (‰)	-20.7±1.1	-19.6±1.3	-26.6±1.3	-26.8±1.0	-26.9±1.4	-24.9±0.7
	-22 to -19.7	-21.9 to -17.6	-27.6 to -24.0	-28.8 to -25.3	-27.9 to -25.9	-25.7 to -23.4
DIC ($\mu mol\ L^{-1}$)	1,100±180	1,520±490	1,500±550	2,830±1,080	1,160±315	2,140±1,200
	930-1,300	820-2,590	570-2,040	1,650-5,370	940-1,380	1,020-4,480
DOC ($\mu mol\ L^{-1}$)	420±120	550±140	2,230±1,440	740±380	310±50	420±100
	320-590	340-880	575-3,670	310-1,720	275-350	310-620

Tab. 3. Values of carbon and ancillary parameters throughout sampling period (Jan. 2014-Jul. 2015) in different types of groundwater across hydrological seasons. Numbers between brackets are corresponding to the sampling size. For each parameter, the table showed the average±standard deviations and the range. We defined six groups that are Cropland_HF/Cropland_BF, Forest_HF/Forest_BF and Riparian_HF/Riparian_BF corresponding to groundwaters during high flow (HF) or base flow (BF); in either cropland, forest or riparian forest.

	First-order streams			
	Cropland_HF (22)	Cropland_BF (37)	Forest_HF (23)	Forest_BF (55)
pH	5.9±0.3	6.1±0.4	5.7±0.6	6.1±0.4
	5.4-6.6	5.5-7.0	4.2-6.8	5.0-6.9
Temperature (°C)	10.2±1.6	15.7±3.9	9.0±1.9	14.6±3.3
	6.4-12.1	9.1-25.8	4.8-12	8.1-22.1
EC ($\mu S\ cm^{-1}$)	230±50	220±60	110±20	120±30
	145-340	75-370	80-150	70-200
NO_3^- ($\mu mol\ L^{-1}$)	420±220	290±170	95±70	65±70
	180-950	8.5-705	0-275	0-275
NH_4^+ ($\mu mol\ L^{-1}$)	7.0±8.4	5.5±6.0	1.7±1.7	1.7±1.7
	0.5-38.7	0-25.3	0.3-7.8	0-6.9
Fe^{2+} ($\mu mol\ L^{-1}$)	6.7±3.8	5.4±4.7	5.7±3.0	8.8±14.0
	1.6-15.7	0.1-22	2.6-13.6	0.6-57.1
O_2 ($\mu mol\ L^{-1}$)	290±50	290±40	300±40	270±60
	190-400	160-370	210-370	110-360
CH_4 ($nmol\ L^{-1}$)	580±1,080	390±880	185±190	270±340
	30-4,380	20-4,900	40-980	20-2,370
pCO_2 (ppmv)	5,200±2,370	4,040±2,790	4,200±2,430	5,200±5,100
	1,040-10,740	1,220-14,080	1,240±11,690	1,010-27,200
TA ($\mu mol\ L^{-1}$)	105±50	100±50	70±40	95±55
	40-300	30-255	35-195	30-280
δ^{13}C-DIC (‰)	-20.6±3.9	-16.8±2.4	-22.1±2.5	-18.9±2.3
	-27.6 to -11.3	-22.3 to -12.4	-27.6 to -16.8	-23.1 to -14.0
DIC ($\mu mol\ L^{-1}$)	380±130	280±120	300±150	330±230
	1,000-650	90-600	150-750	120-1,280
DOC ($\mu mol\ L^{-1}$)	750±400	520±230	540±305	450±220
	300-2,290	220-1,520	260-1725	190-1540
TSM ($mg\ L^{-1}$)	9.3±11.5	3.1±4.9	2.8±1.7	2.1±1.7
	0.9-51	0.1-27	0.5-6.6	0.4-8.2
POC (%)	26±10	30±10	29±8	29±10
	15-48	16-48	20-50	12-80
POC ($\mu mol\ L^{-1}$)	190±250	65±100	65±40	40±30
	0-1100	0.3-540	0-170	0.5-140

Tab. 4. Values of carbon and ancillary parameters throughout sampling period (Jan. 2014-Jul. 2015) in different types of streams across hydrological seasons. Numbers between brackets are corresponding to the sampling size. For each parameter, the table showed the average±standard deviations and the range. We defined four groups that are Cropland_HF/Cropland_BF, Forest_HF/Forest_BF corresponding to streams during high flow (HF) or base flow (BF); in either cropland-affected or forest-dominated land use.

Figure 1: Land use map of the Leyre catchment showing river network and the sampling locations of groundwaters and streams.

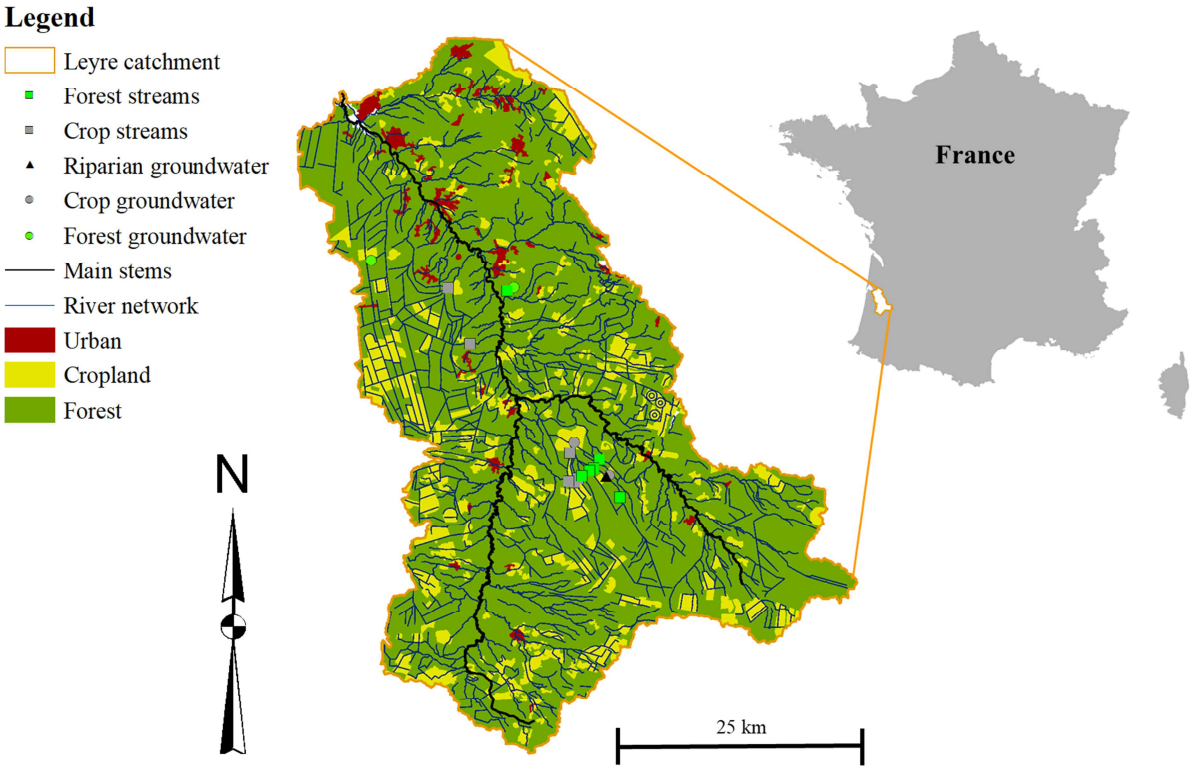

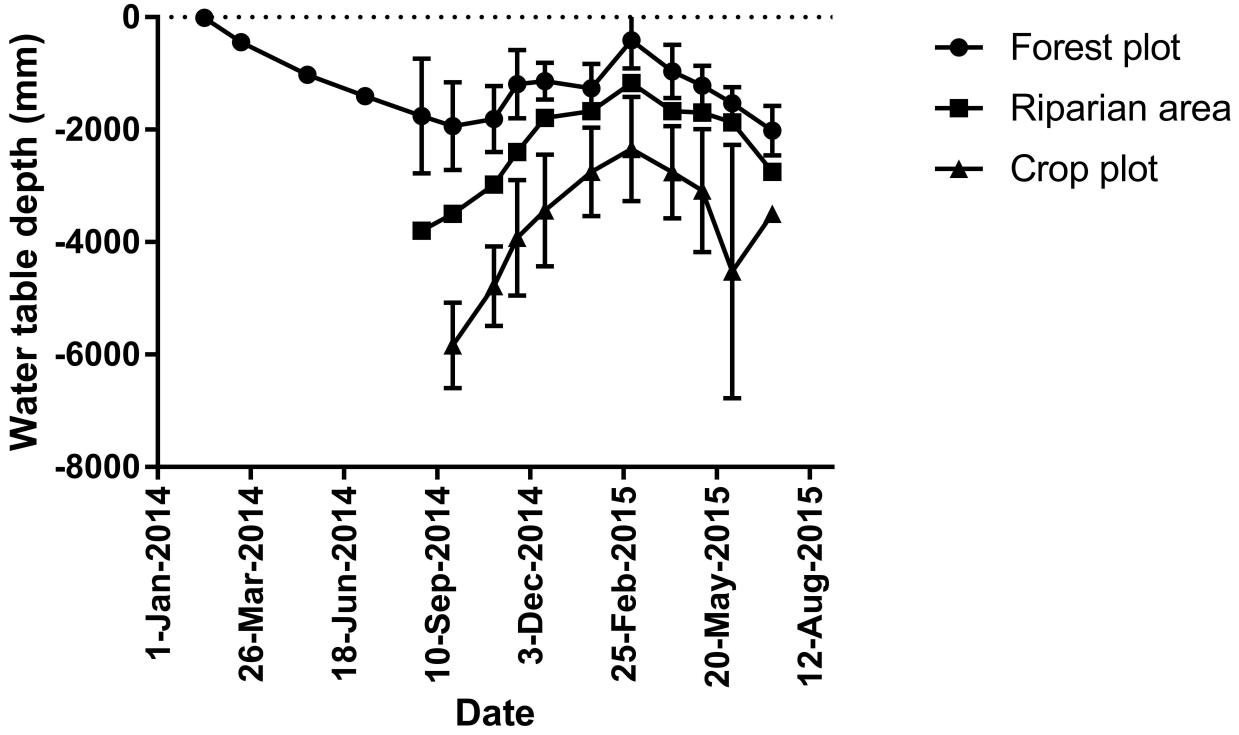

Figure 2: Water table depth during the sampling period (Jan. 2014-Jul. 2015) across land use in the Leyre catchment. The water table in riparian area is the water table at P1 (Tab. 1). The water table in crop plot is the average±standard deviations of water tables at P2 and P3 (Tab. 1). The water table in forest plot is the average±standard deviations of water tables at P4 and P5 (Tab. 1).

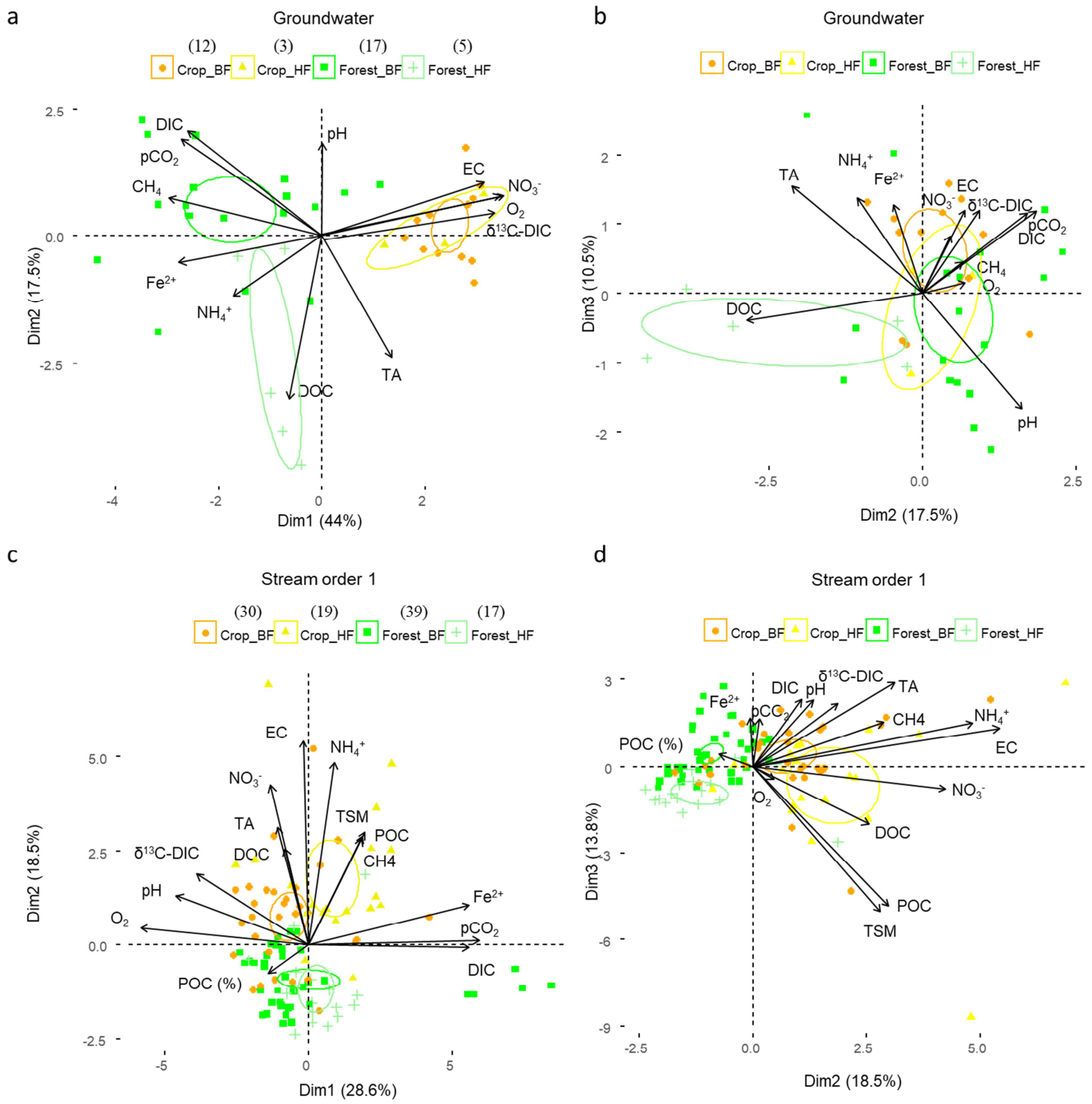

Figure 3: Principal component analysis (PCA) of shallow groundwater dataset (a-b) and first-order streams dataset (c-d). We represented only the first three dimensions. Numbers between brackets are corresponding to the sampling size. The sampling size in the PCAs did not correspond exactly to the sampling size in Tables 3 and 4 because R software deletes stations from the analysis with a missing value for one parameter. In these PCAs, we used all the quantitative variables measured in this study. In each PCA, we plotted as well the individuals separated in four groups. The first group corresponds to cropland-affected samples during high flow (Crop_HF), the second group corresponds to cropland-affected samples during base flow (Crop_BF), the third group corresponds to forest-dominated samples during high flow (Forest_HF) and the fourth group corresponds to forest-dominated samples during base flow (Forest_BF).

The mean value of each qualitative group has 95% chance to be within the corresponding confidence ellipse.

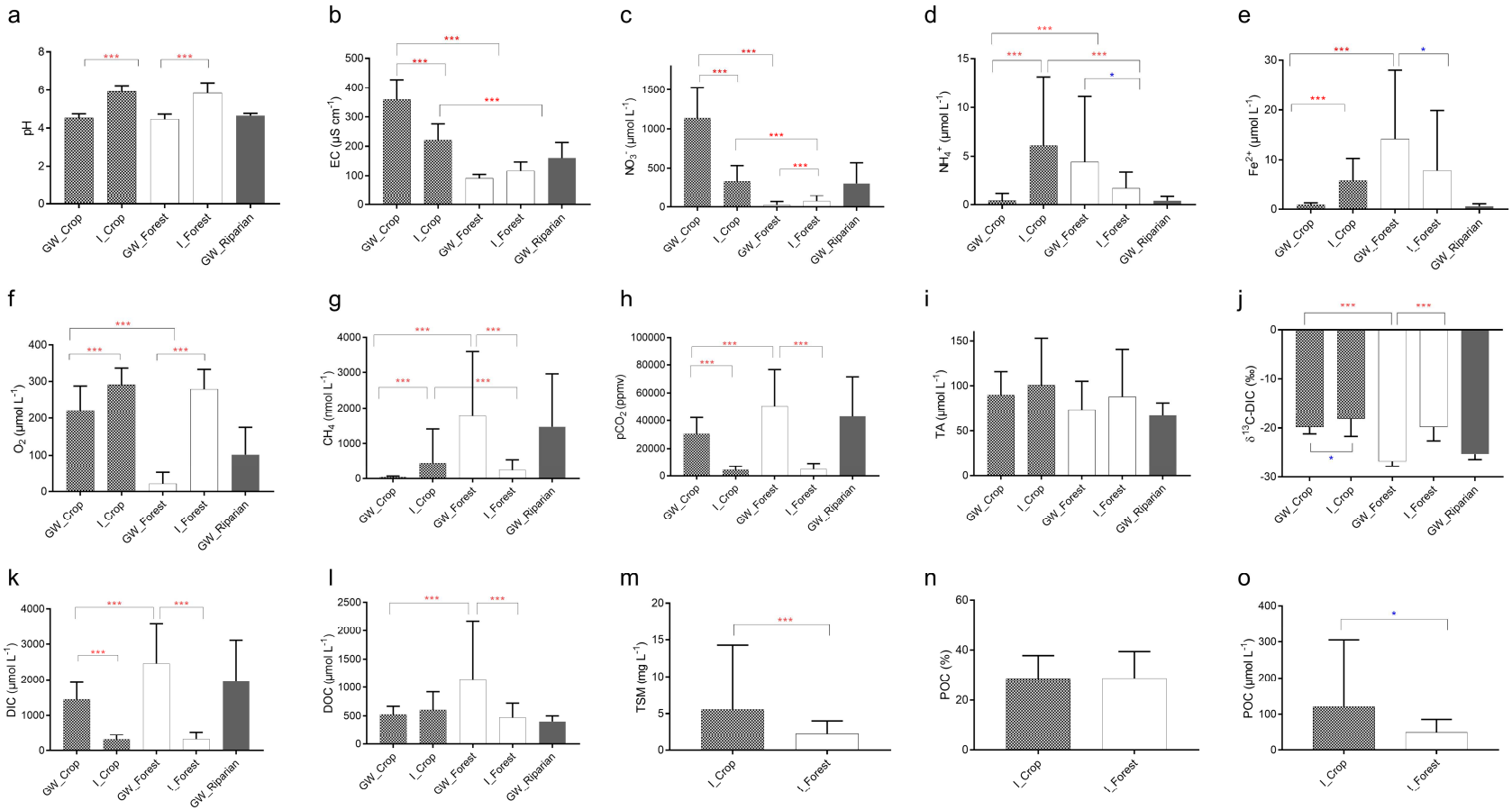

Figure 4: Values of carbon and ancillary parameters throughout the sampling period (Jan. 2014-Jul. 2015) in groundwater and streams across land use. Histograms represent the mean with standard deviations of a given parameter. We defined four groups that are GW_Forest/GW_Crop and I_Forest/I_crop corresponding to groundwaters and streams order 1 either dominated by forests or croplands. A fifth group is GW_Riparian and corresponding to riparian groundwater. Then, based on Mann-Whitney statistical analysis, we compared GW_Crop VS I_Crop, GW_Forest VS I_Forest, GW_Crop VS GW_Forest, I_Crop VS I_Forest. Three red stars (***) indicate that data were significantly different with $p<0.001$. One blue star (*) indicates that data were significantly different with $p<0.05$. No stars indicate that data were not significantly different ($p>0.05$).

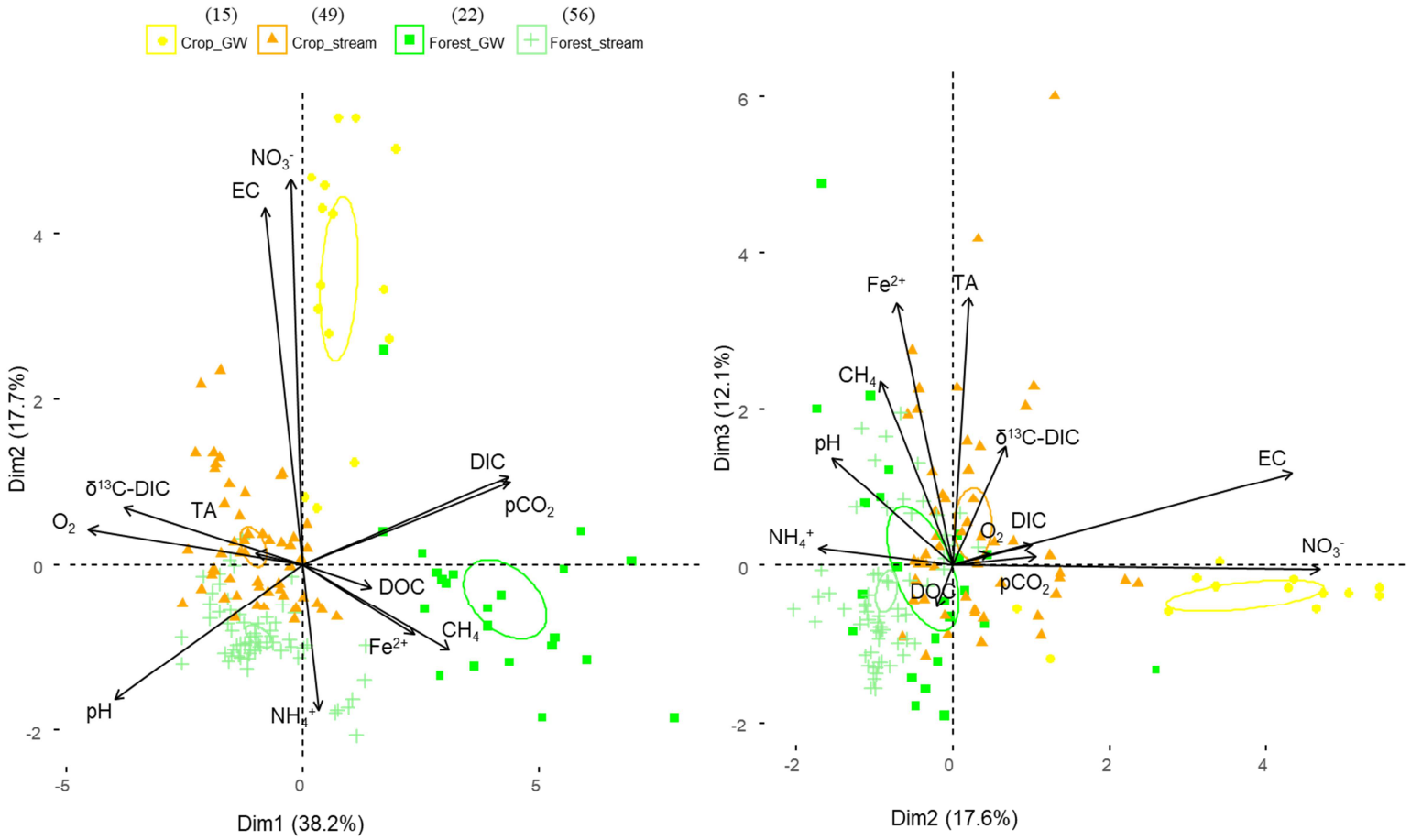

Figure 5: Principal component analysis (PCA) of shallow groundwater and stream datasets. We represented only the first three dimensions. Numbers between brackets are corresponding to the sampling size. The sampling size in the PCA did not correspond exactly to the sampling size in Table 2 because R software deletes stations from the analysis with a missing value for one parameter. In these multivariate statistical analyses, we used all the quantitative variables measured in this study. We defined four groups that are Crop_GW/Forest_GW and Crop_stream/Forest_stream, which are corresponding to groundwater and streams order 1, either dominated by forests or croplands. The mean value of each qualitative group has 95% chance to be within the corresponding confidence ellipse

Figure 6: Scatter plots of (a) CO_2 (ppmv) vs. O_2 (µmol L^{-1}), (b) CO_2 (ppmv) vs. DOC (µmol L^{-1}), (c) CH_4(nmol L^{-1}) vs. O_2 (µmol L^{-1}), (d) CH_4 vs. DOC (µmol L^{-1}), (e) CH_4(nmol L^{-1}) vs. CO_2 (ppmv), and (f) O_2 (µmol L^{-1}) vs. DOC (µmol L^{-1}), in all sampled groundwater and streams

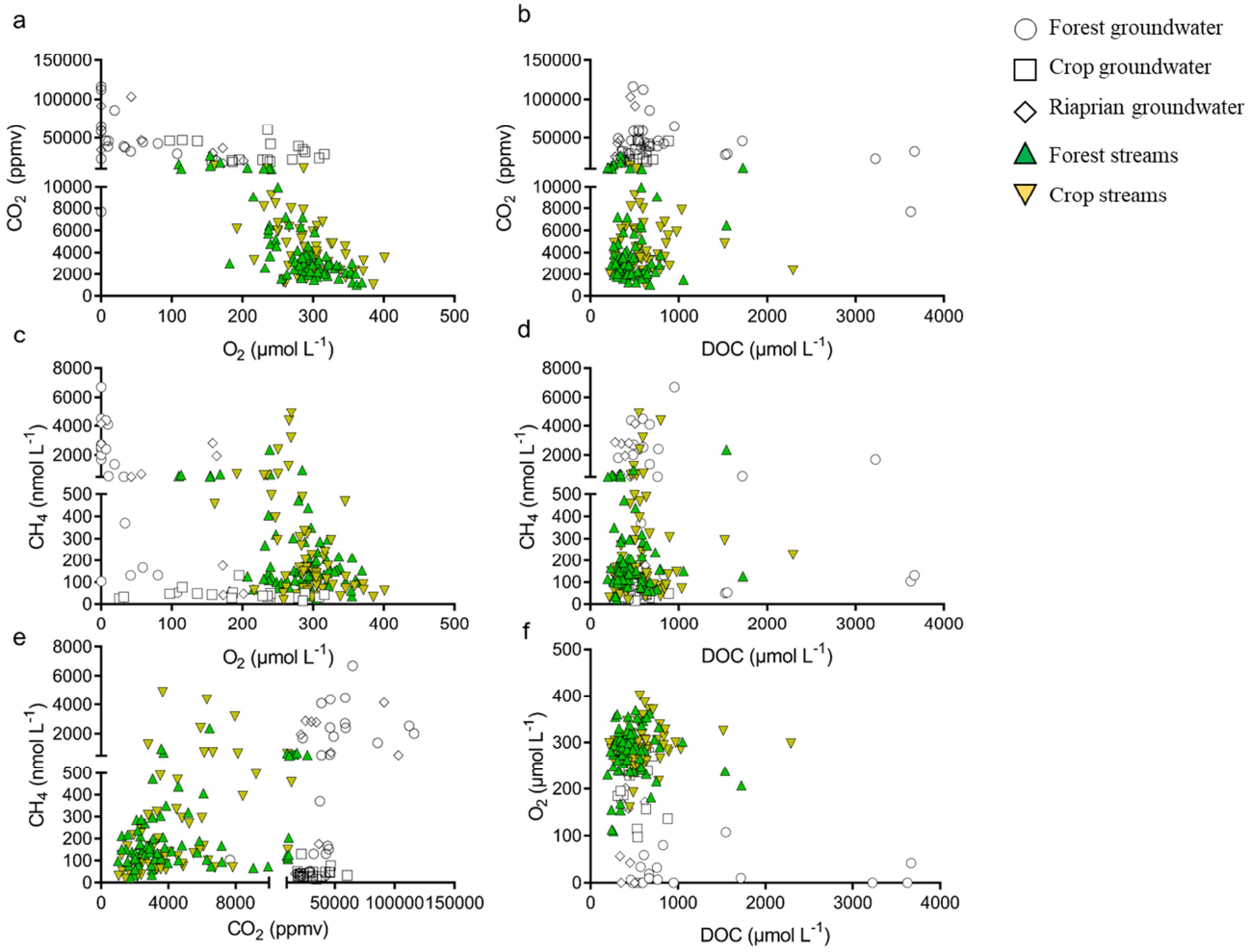

Figure 7: Scatter plots of (a) O_2 (µmol L^{-1}) vs. NO_3^- (µmol L^{-1}), (b) O_2 (µmol L^{-1}) vs. NH_4^+ (µmol L^{-1}), (c) CH_4 (µmol L^{-1}) vs. NO_3^- (µmol L^{-1}), (d) CH_4 (µmol L^{-1}) vs.DOC (µmol L^{-1}), (e) DOC (µmol L^{-1}) vs. NO_3^- (µmol L^{-1}), and (f) O_2 (µmol L^{-1}) vs. Fe^{2+}(µmol L^{-1}), in all sampled groundwater and streams.

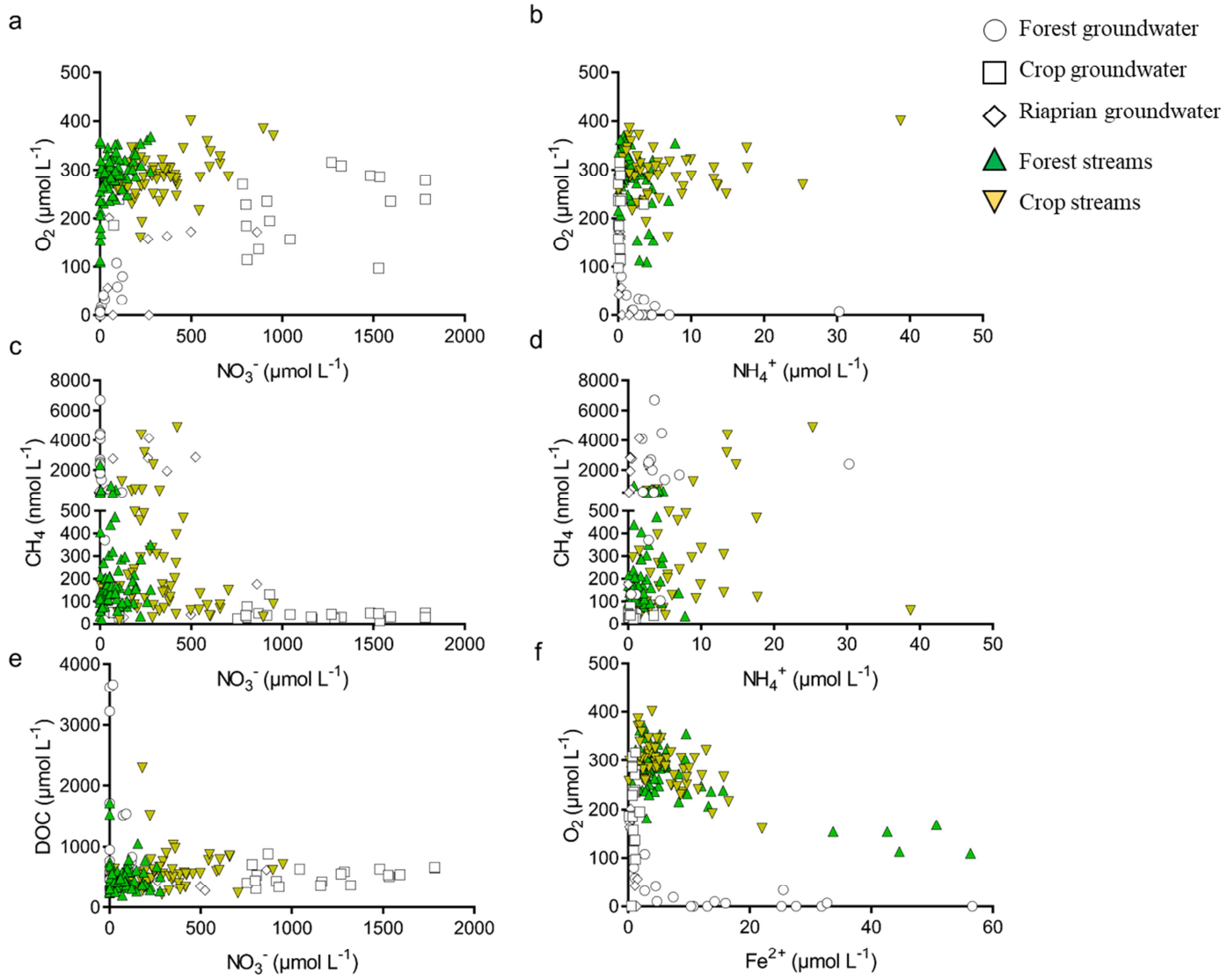

Supplementary Material

Seasons	Date	Groundwaters			Streams
		P5	P1, P2, P3	P4	
HF	29/01/2014				X
HF	12/02/2014	X			
HF	07/03/2014				X
HF	17/03/2014	X			
BF	24/04/2014				X
BF	16/05/2014	X			
BF	21/05/2014				X
BF	25/06/2014				X
BF	17/072014	X			X
BF	27/08/2014	X	X		X
BF	24/09/2014	X	X		X
BF	31/10/2014	X	X		X
BF	21/11/2014	X	X		X
BF	16/12/2014	X	X		X
HF	27/01/2015	X	X	X	X
HF	04/03/2015	X	X	X	X
BF	10/04/2015	X	X	X	X
BF	07/05/2015	X	X	X	X
BF	03/06/2015	X	X	X	X
BF	09/07/2015	X	X	X	X

Table S1: Sampling dates of groundwaters and streams. X corresponds to a sampling. HF and BF are corresponding to high flow and base flow periods, respectively.

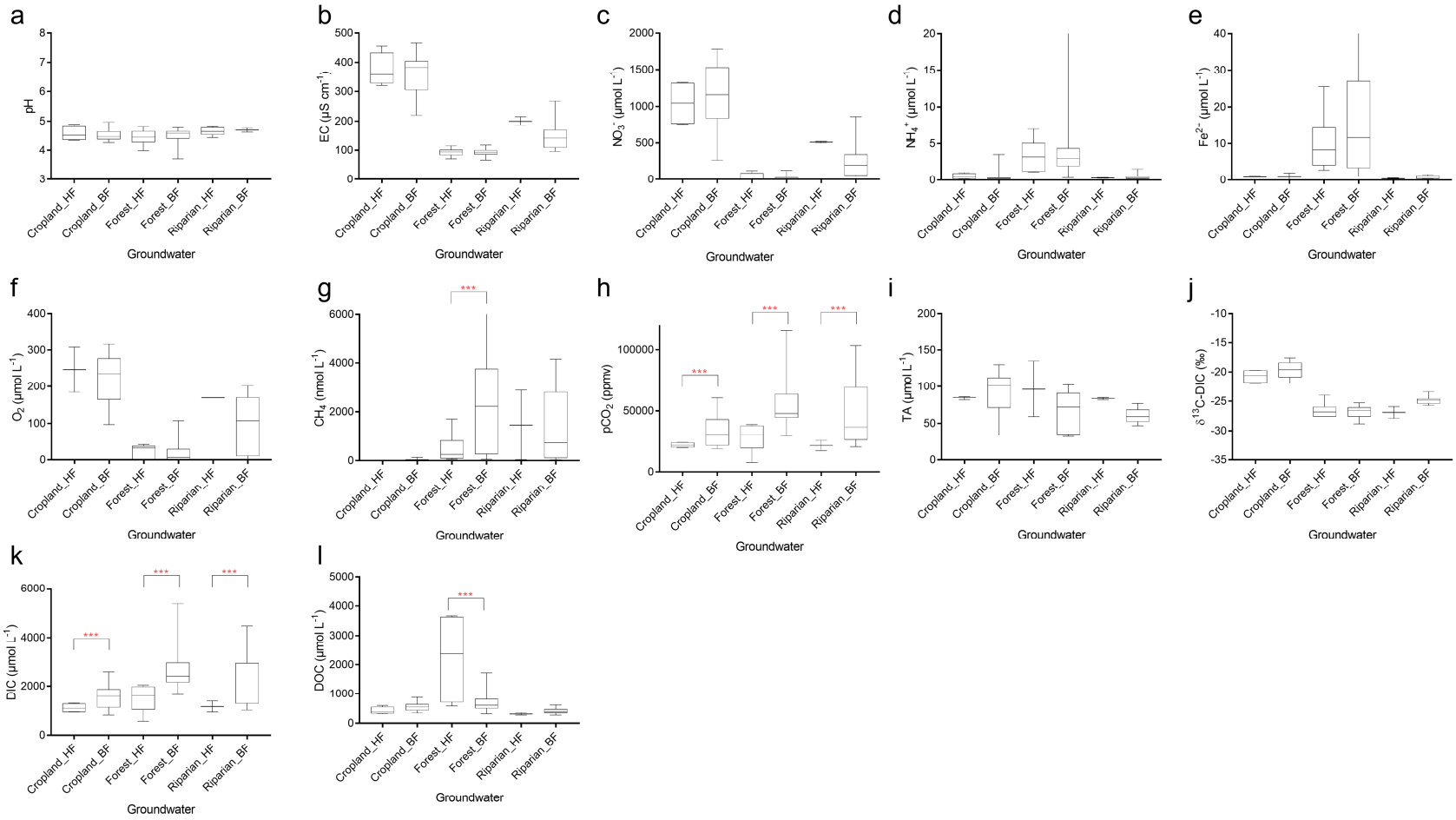

Fig. S2. Values of carbon and ancillary parameters throughout the sampling period (Jan. 2014-Jul. 2015) in groundwaters across hydrological seasons and land use. Box-plots represent the median (black bar) and the extreme (min-max) values. We defined six groups that are Cropland_HF/Cropland_BF, Forest_HF/Forest_BF and Riparian_HF/Riparian_BF corresponding to groundwater during high or base flow; in either cropland, forest or riparian forest. Then, based on Mann-Whitney statistical analysis, we compared Cropland_HF vs. Cropland_BF,

Forest_HF vs. Forest_BF and Riparian_HF vs. Riparian_BF. Three red stars (***) indicate that data were significantly different with $p<0.001$. One blue star (*) indicates that data were significantly different with $p<0.05$. No stars indicate that data were not significantly different ($p>0.05$)

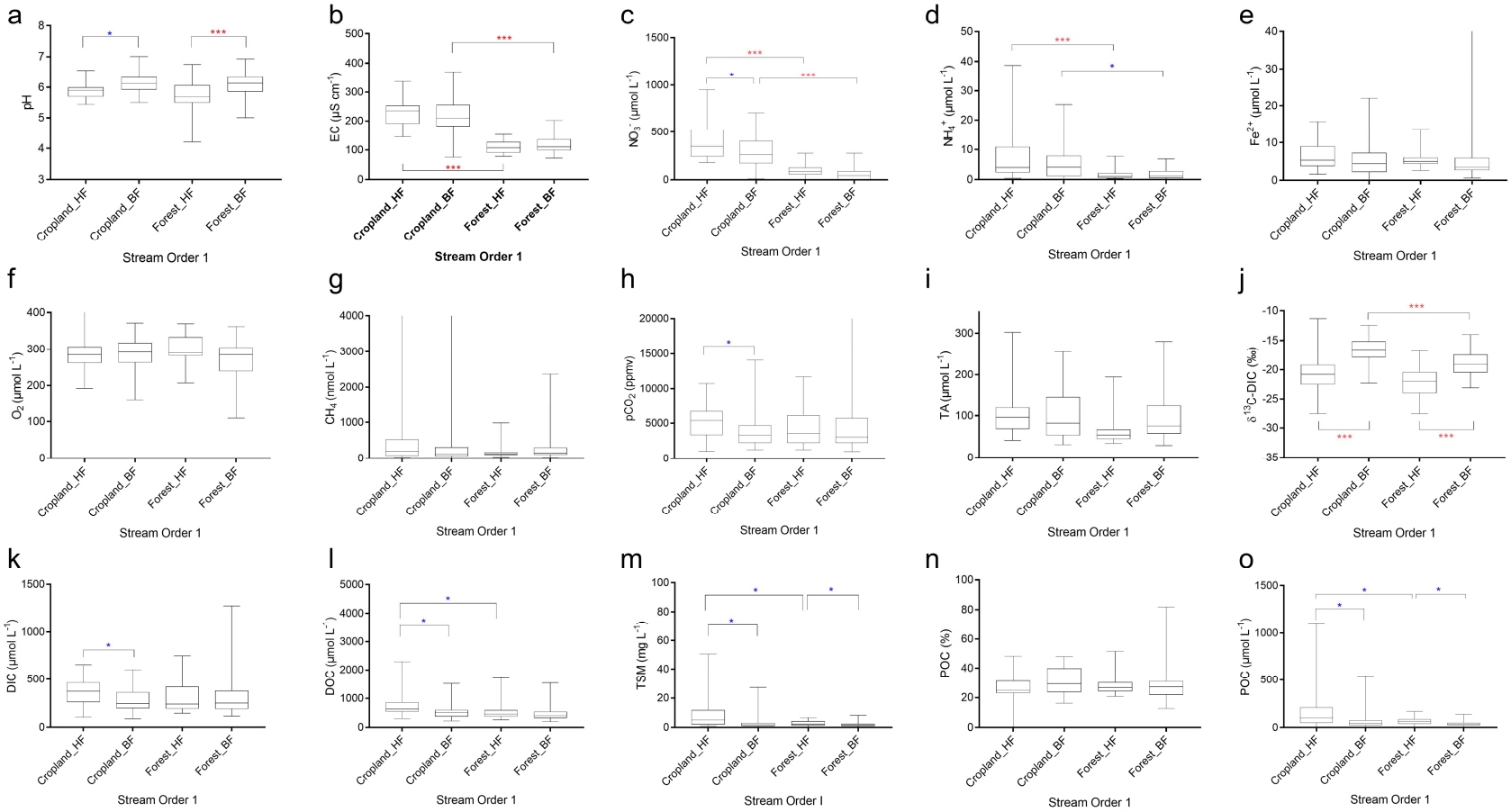

Figure S3. Values of carbon and ancillary parameters throughout the sampling period (Jan. 2014-Jul. 2015) in streams across hydrological seasons and land use Box-plots represent the median (black bar) and the extreme (min-max) values. We defined four groups that are Cropland_HF/Cropland_BF, Forest_HF/Forest_BF corresponding to streams during high or base flow periods; in either cropland-affected or forest-dominated land use. Then, based on Mann-Whitney statistical analysis, we compared compared Cropland_HF vs. Cropland_BF, Forest_HF vs. Forest_BF, Cropland_BF vs. Forest_HF and Cropland_BF vs. Forest_BF. Three red stars (***) indicate that data were significantly different with $p<0.001$. One blue star (*) indicates that data were significantly different with $p<0.05$. No stars indicate that data were not significantly different ($p>0.05$)

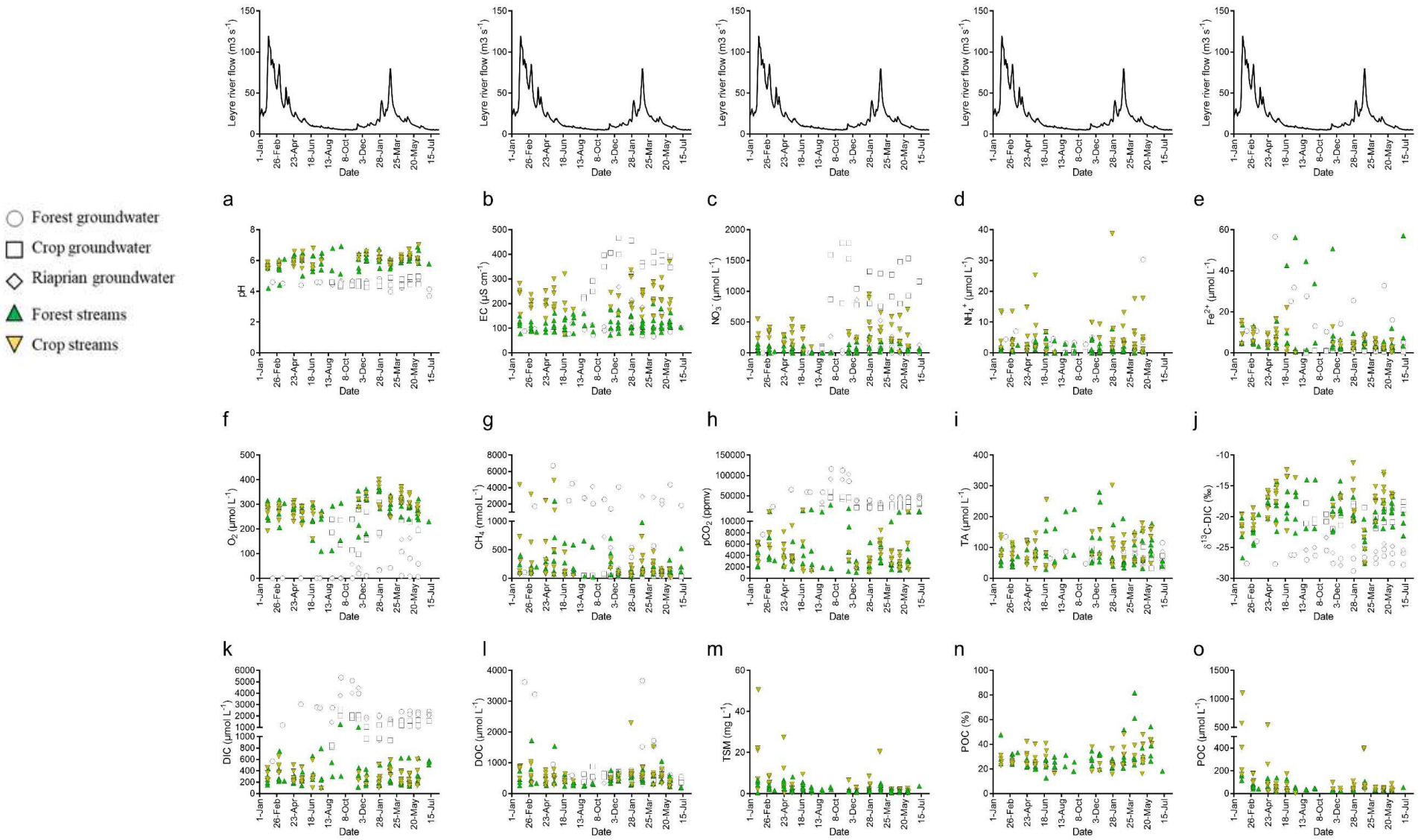

Figure S4: Temporal variations of carbon and ancillary parameters throughout the sampling period (Jan. 2014-Jul. 2015) in all sampled

groundwater and streams. Top panels represent the Leyre River flow (main stem).

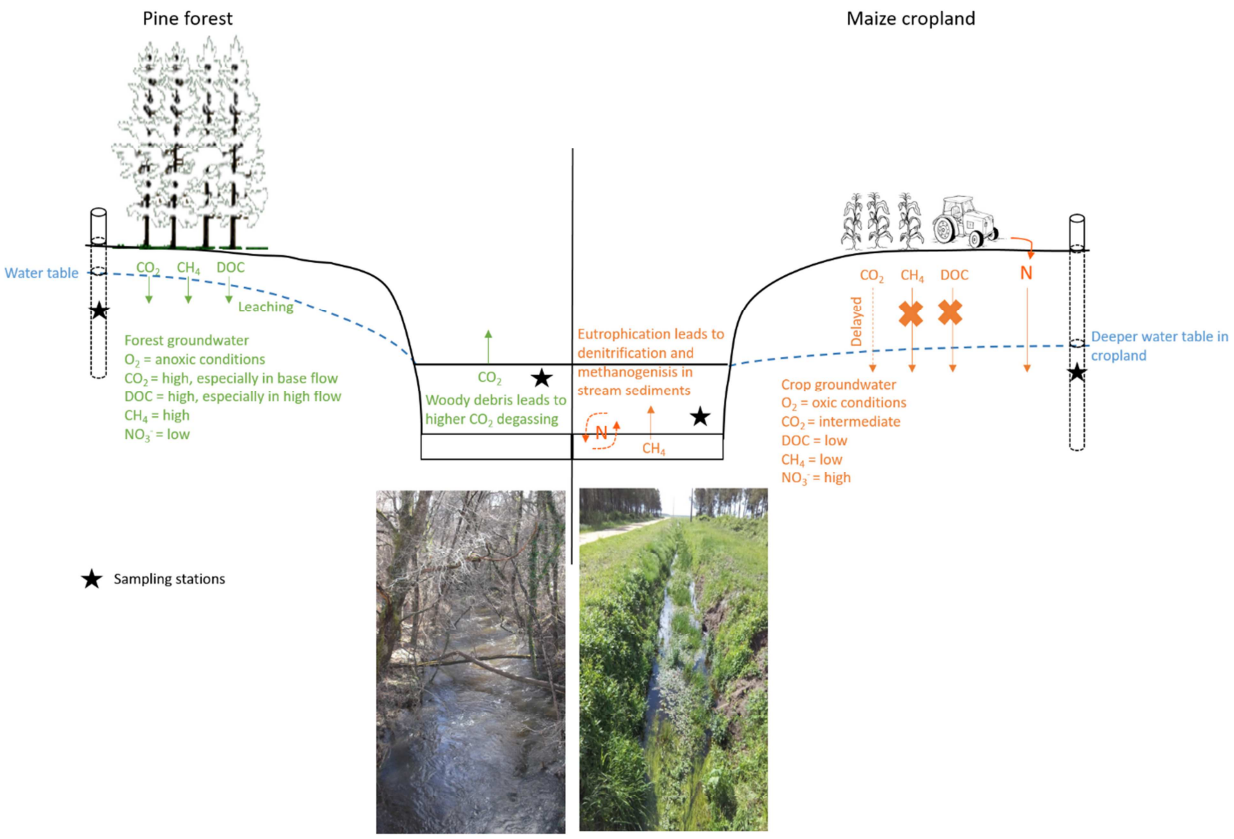
Pine forest
Maize cropland
Water table
CO_2 CH_4 DOC
Leaching
Forest groundwater
O_2 = anoxic conditions
CO_2 = high, especially in base flow
DOC = high, especially in high flow
CH_4 = high
NO_3^- = low
CO_2
Woody debris leads to higher CO_2 degassing
Eutrophication leads to denitrification and methanogenisis in stream sediments
N
CH_4
CO_2 CH_4 DOC
N
Delayed
Deeper water table in cropland
Crop groundwater
O_2 = oxic conditions
CO_2 = intermediate
DOC = low
CH_4 = low
NO_3^- = high
Sampling stations